X-ray Telescopes for

Axions

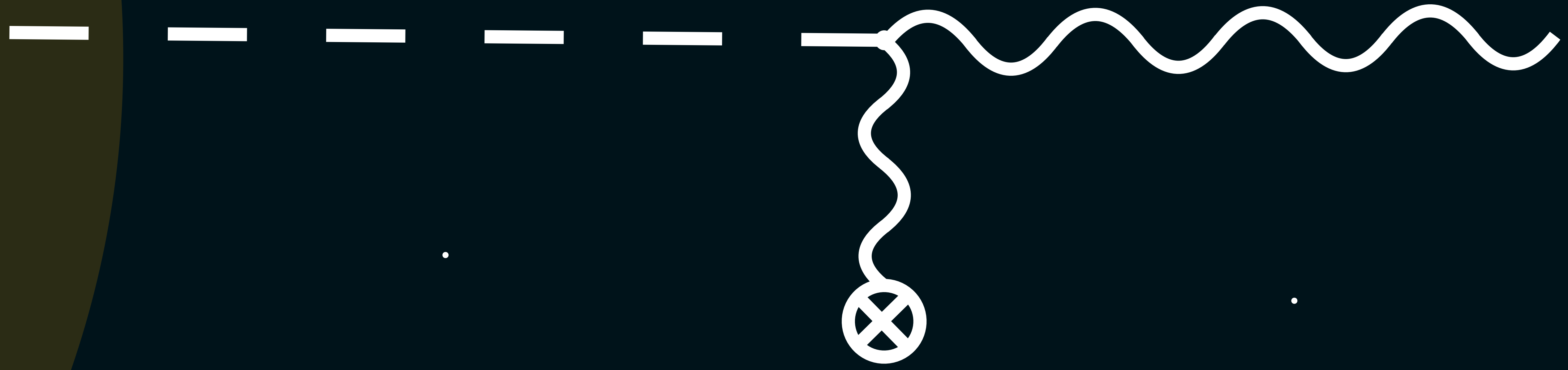

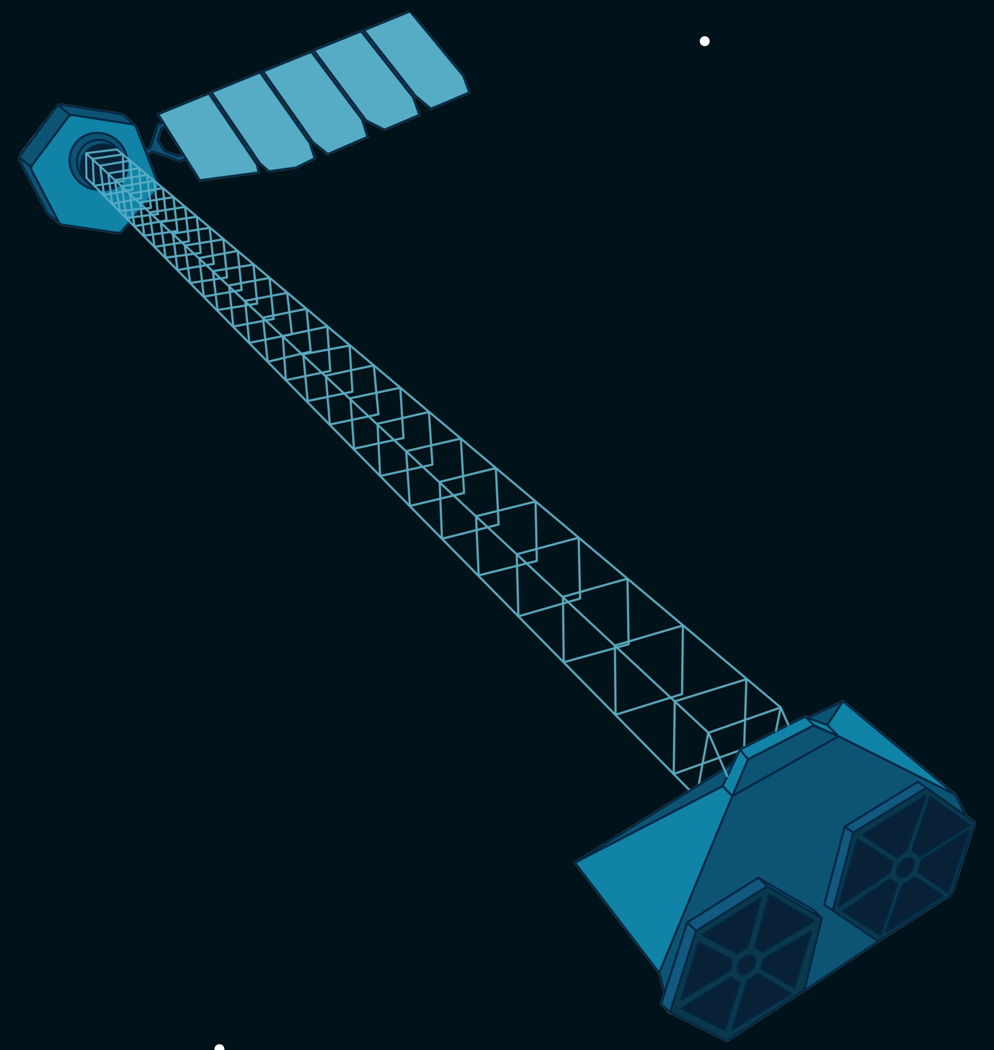

IDM 2026

Francisco Rodríguez Candón

color meets flavor | technische universität dortmund | Universidad Zaragoza 1542 | CAPA

Axion Like Particles (ALPs)

Different
SM Extensions

- Supersimetric Models
- Multidimensional Kaluza-Klein..

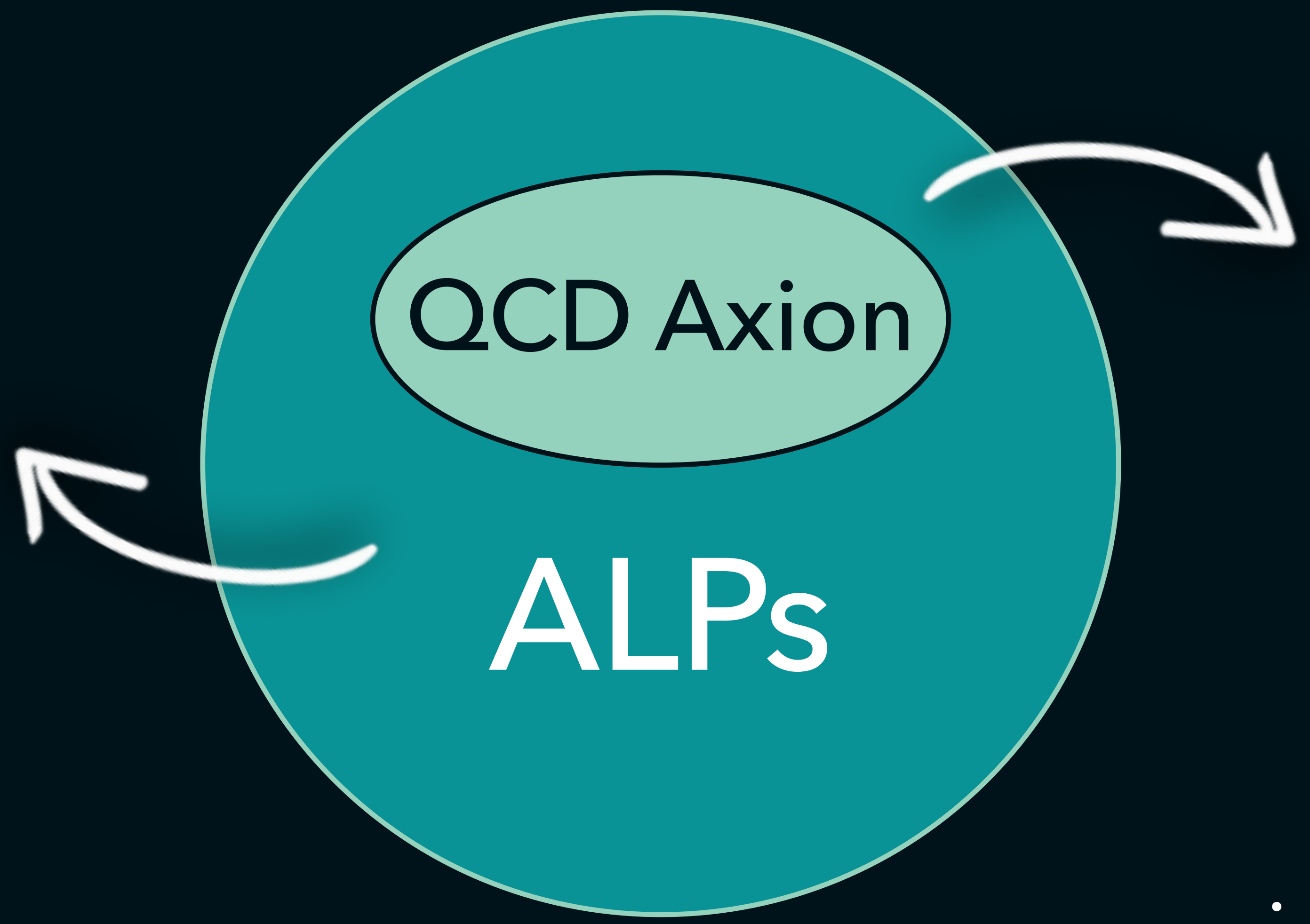

Solution of the
Strong CP Problem

$$\mathcal{L}_{\mathrm{QCD}} \supset \theta \frac{g_s^2}{32\pi^2} G_{\mu\nu}\tilde{G}^{\mu\nu} \qquad |\bar{\theta}_{\mathrm{QCD}}| \lesssim 2 \times 10^{-10}$$

R. D. Peccei and H. R. Quinn
Phys. Rev. Lett. 38 (1977) 1440

$$L_{\mathrm{int}} = \sum_{\psi=e,p,n} \frac{g_{a\psi}}{2m_\psi} \underbrace{\left(\bar{\psi}\gamma^\mu\gamma^5\psi\right)}_{\text{Fermions}} \partial_\mu a - \frac{1}{4} g_{a\gamma} \underbrace{\tilde{F}^{\mu\nu} F_{\mu\nu} a}_{\text{Photons}}$$

Stars as Axion Laboratories

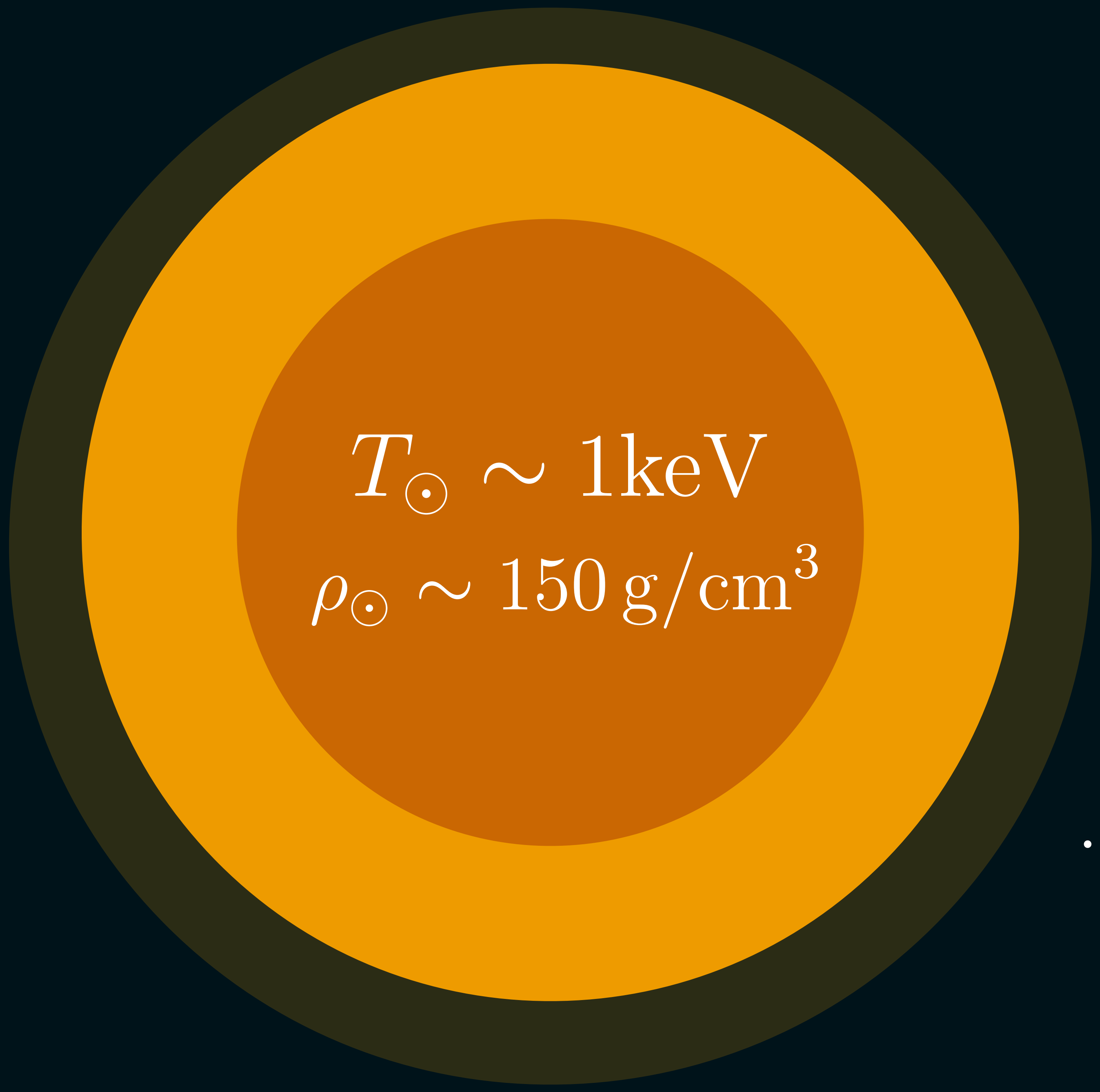

Primakoff Conversion

$$\gamma + Ze \to a + Ze$$

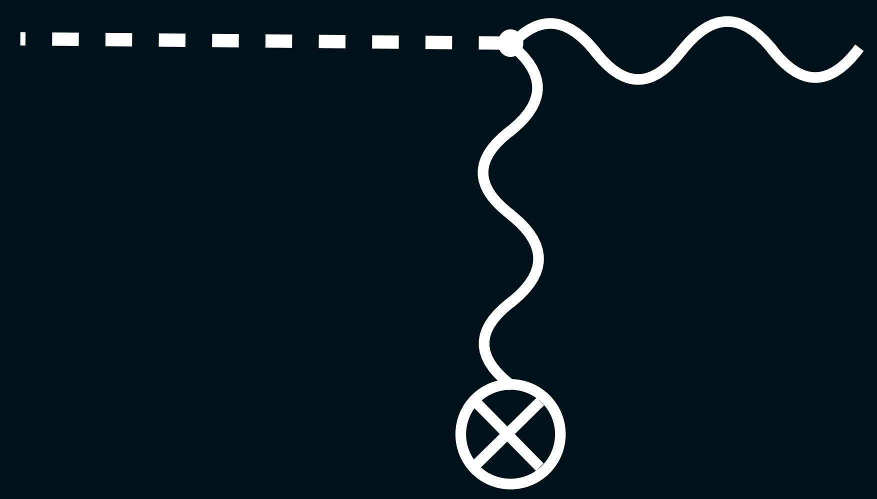

Compton Scatering

$$\gamma + e \to a + e$$

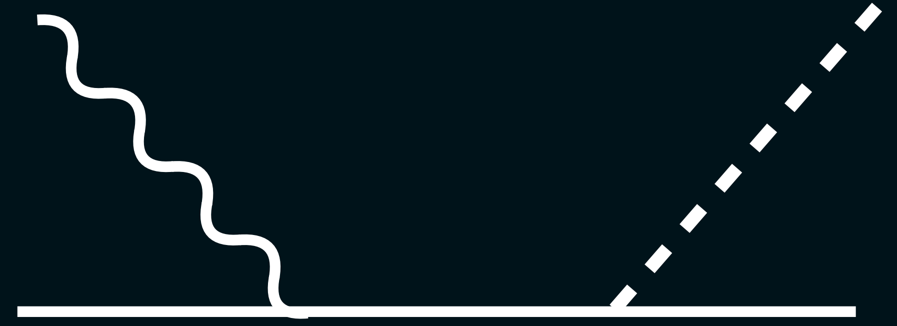

Nucleon Bremsstrahlung

$$N + N \to N + N + a$$

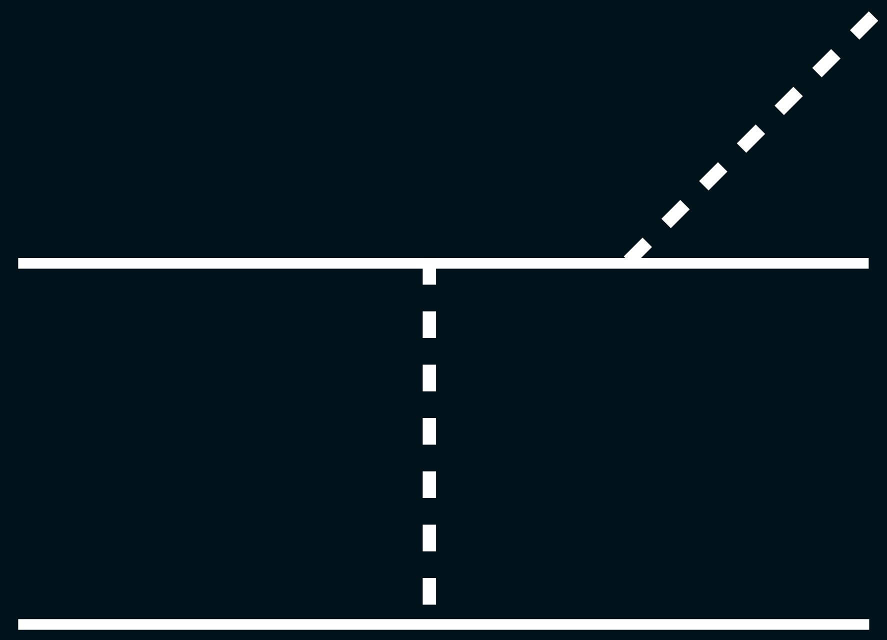

...

$$P_{a\to\gamma} \simeq \left(\frac{g_{a\gamma} B_T L}{2}\right)^2$$

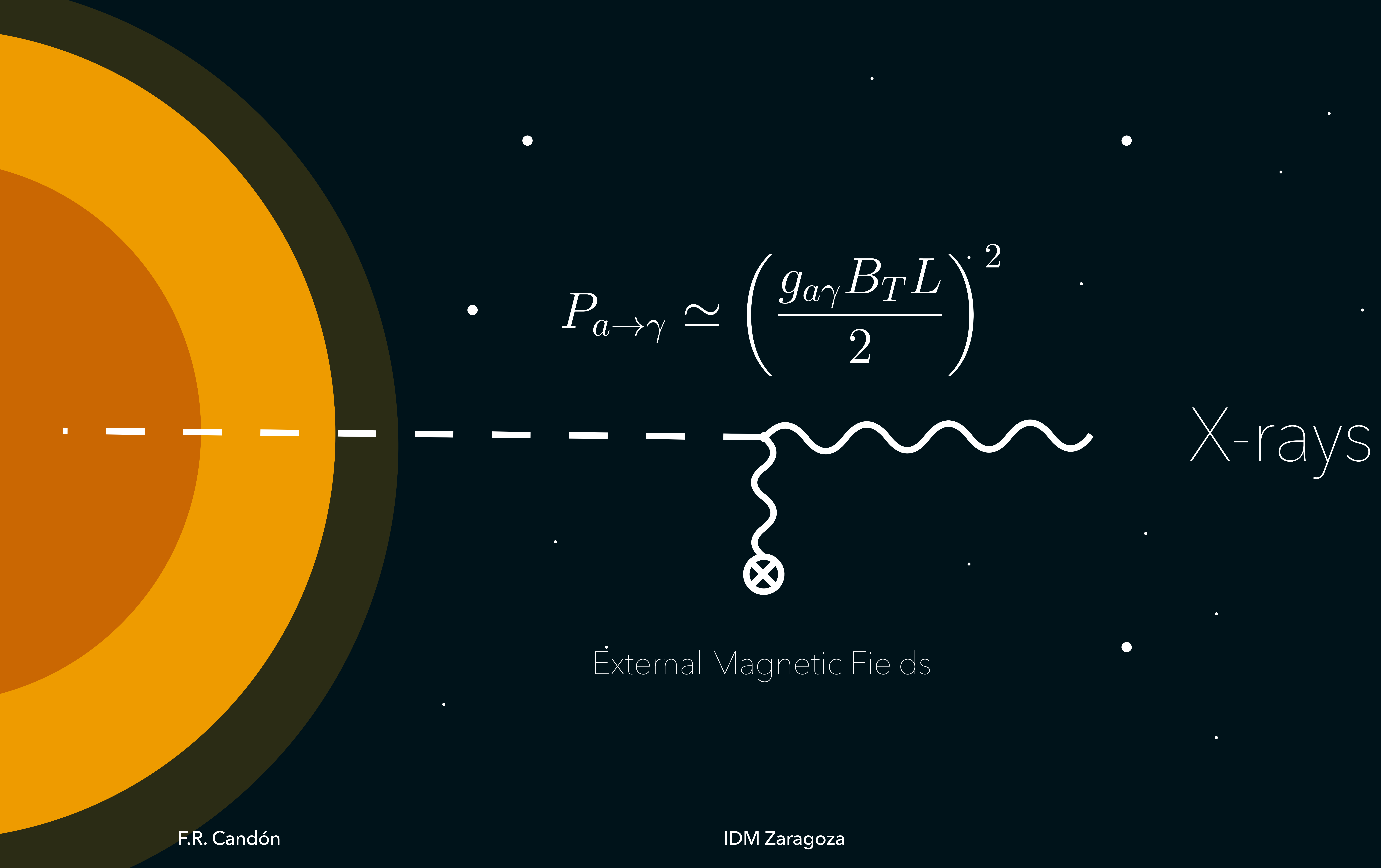

$$P_{a\to\gamma} \simeq \left(\frac{g_{a\gamma} B_T L}{2}\right)^2$$

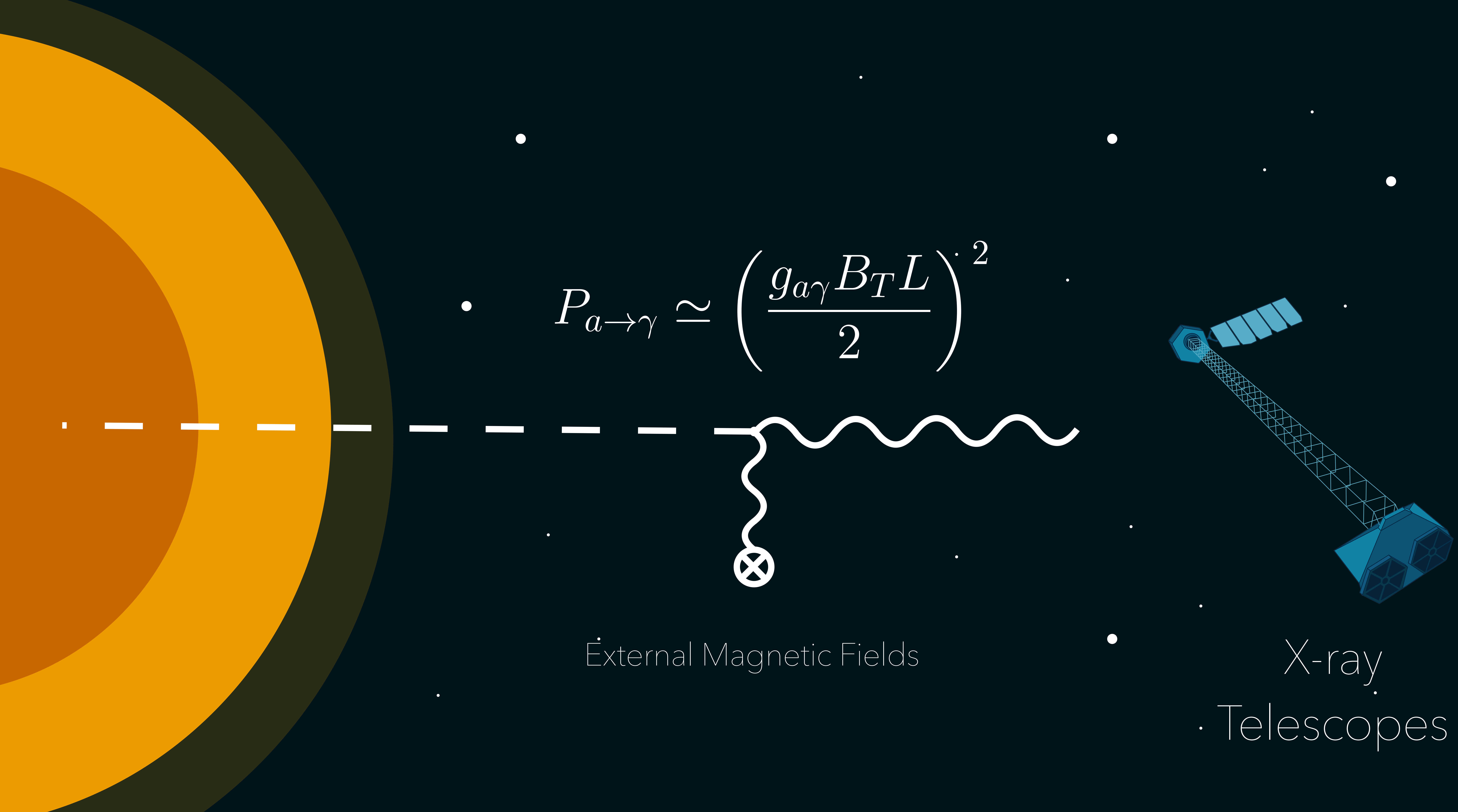

NuSTAR X-ray Telescope

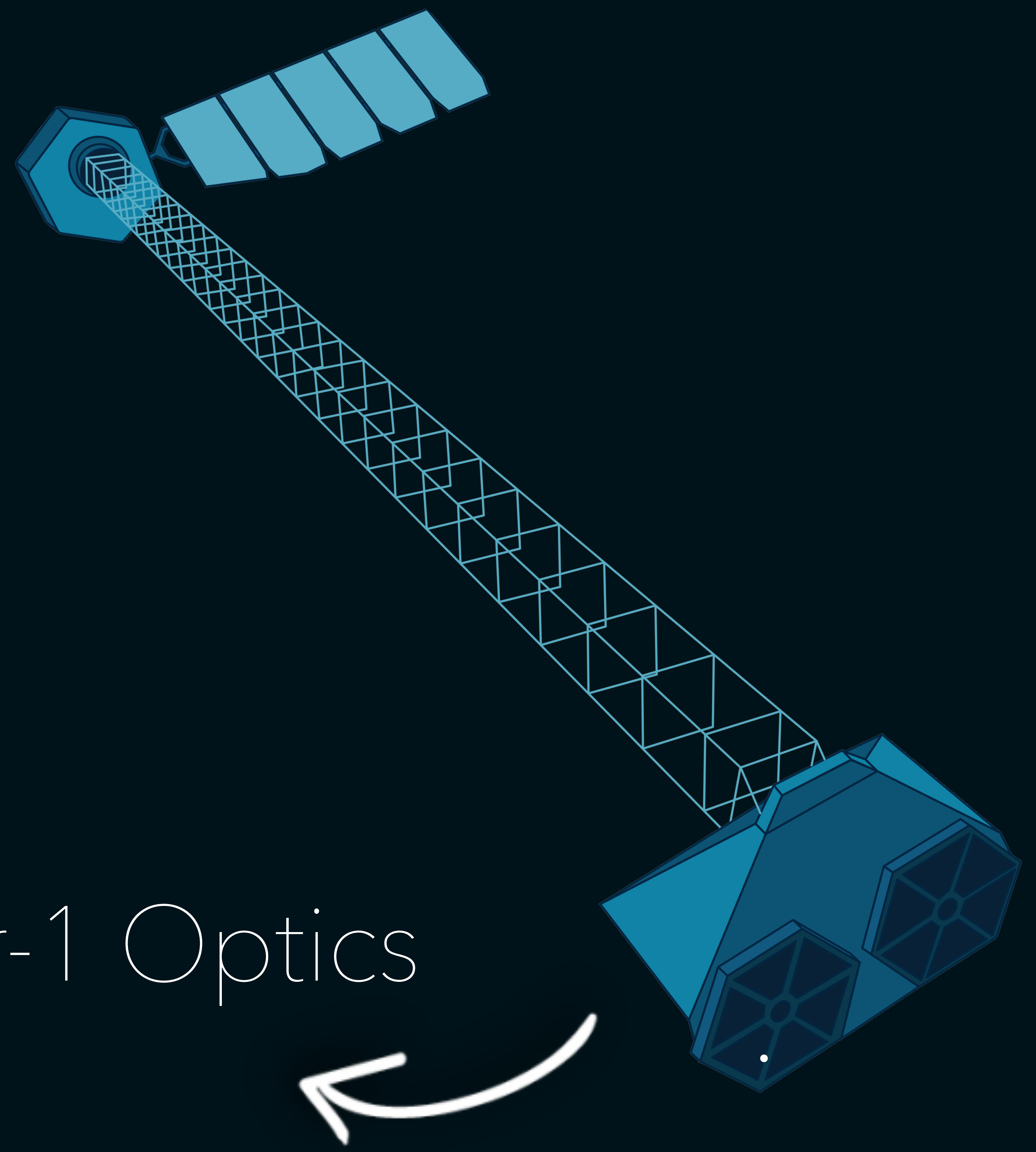

Wolter-1 Optics

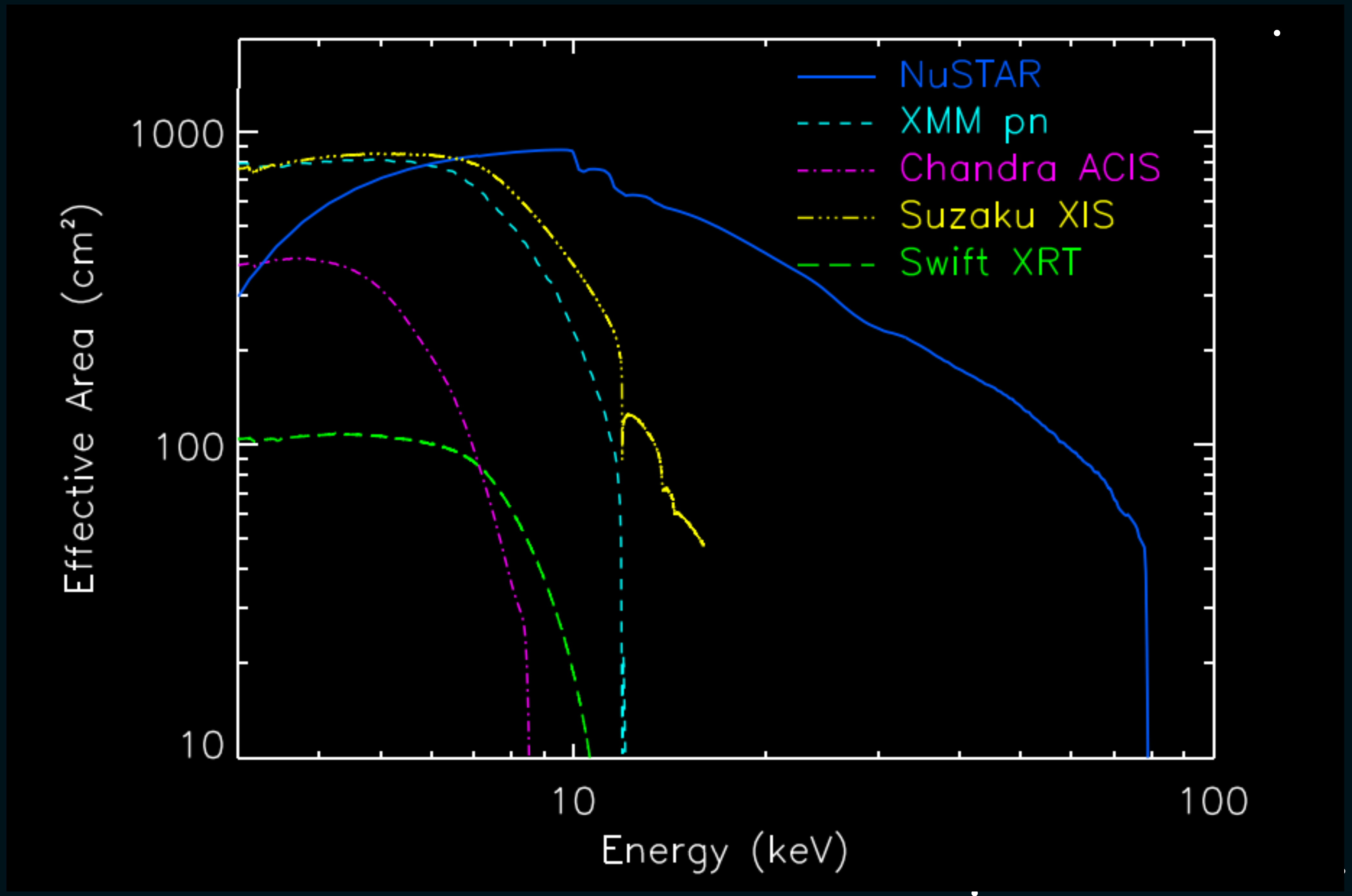

X-ray Telescopes for Axion Searches

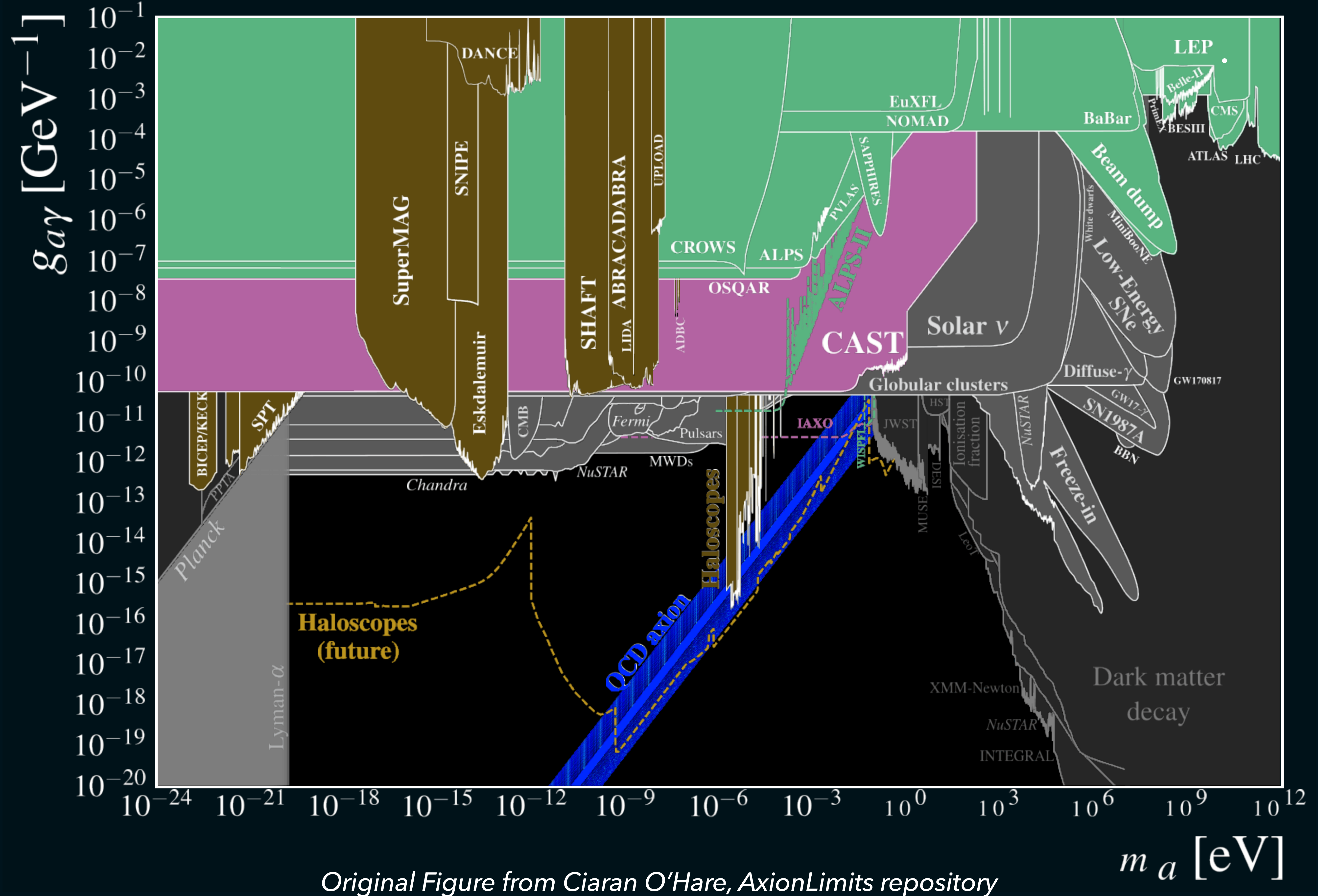

Original Figure from Ciaran O'Hare, AxionLimits repository

X-ray Telescopes for Axion Searches

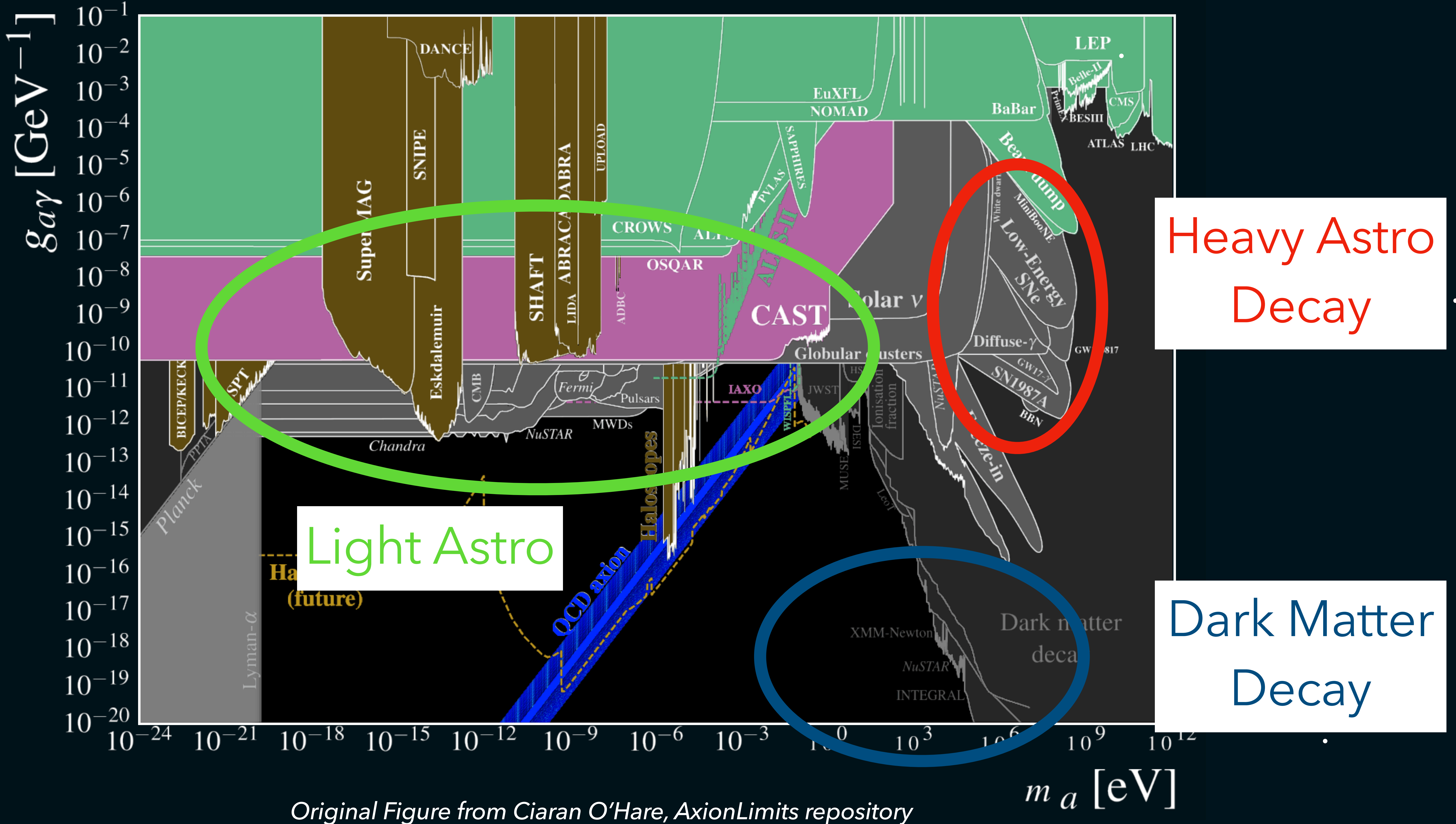

Original Figure from Ciaran O'Hare, AxionLimits repository

The Betelgeuse case

Red Supergiant Star

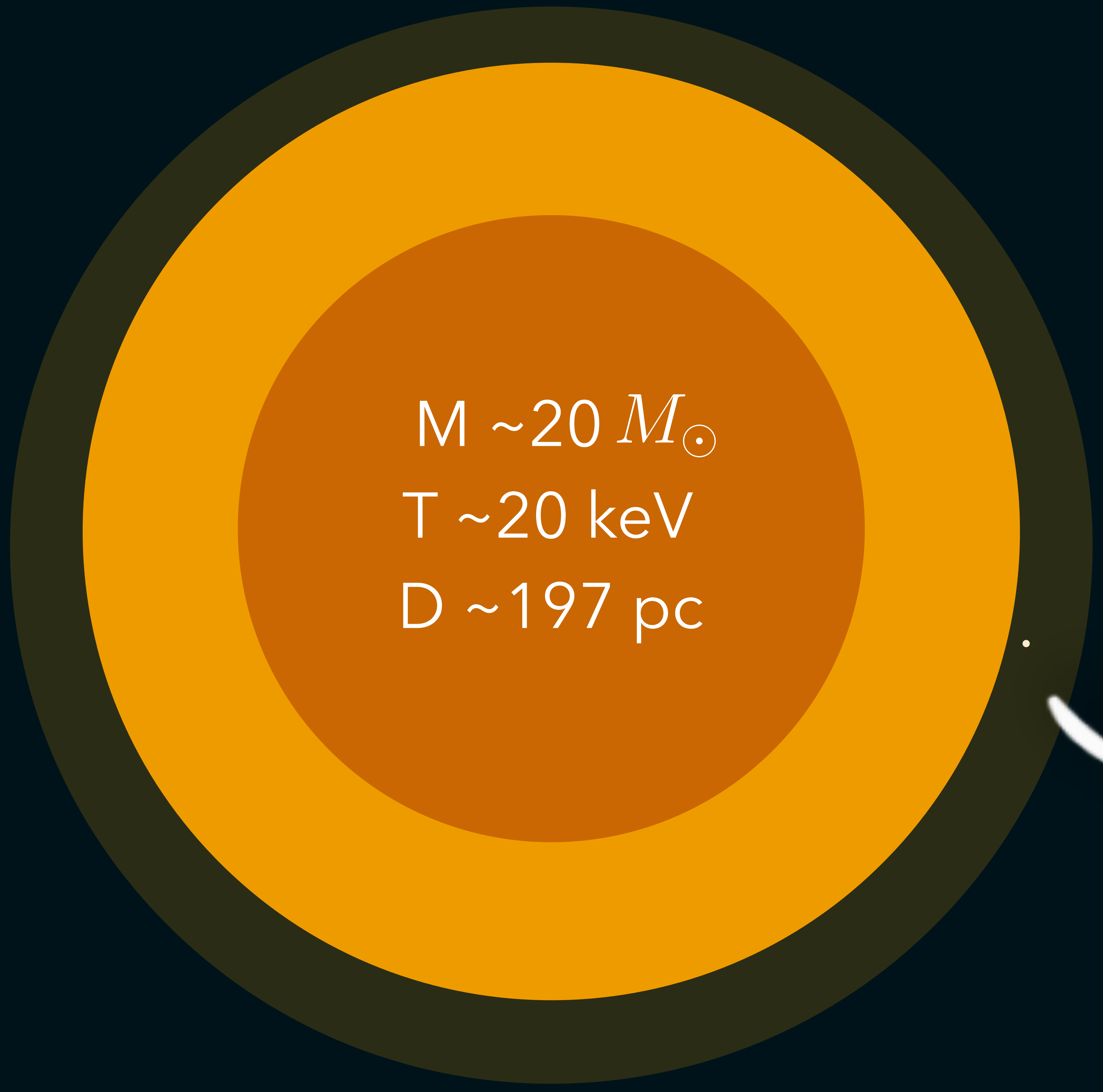

Magnetic dipole (M1) Nuclear transition

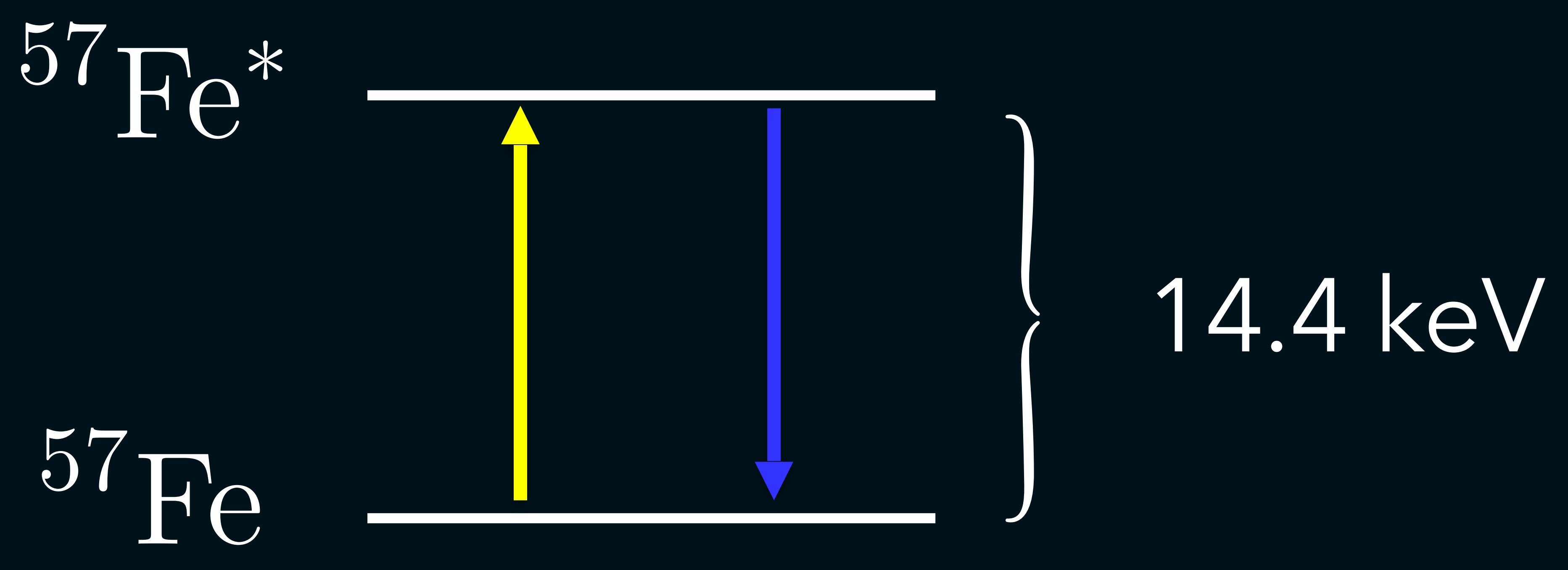

$$\frac{\Gamma_a}{\Gamma_\gamma} = 2.32\,\underbrace{(0.16 g_{ap} + 1.16 g_{an})}_{g_{aN}^{\mathrm{eff}}}$$

The Betelgeuse case

Red Supergiant Star

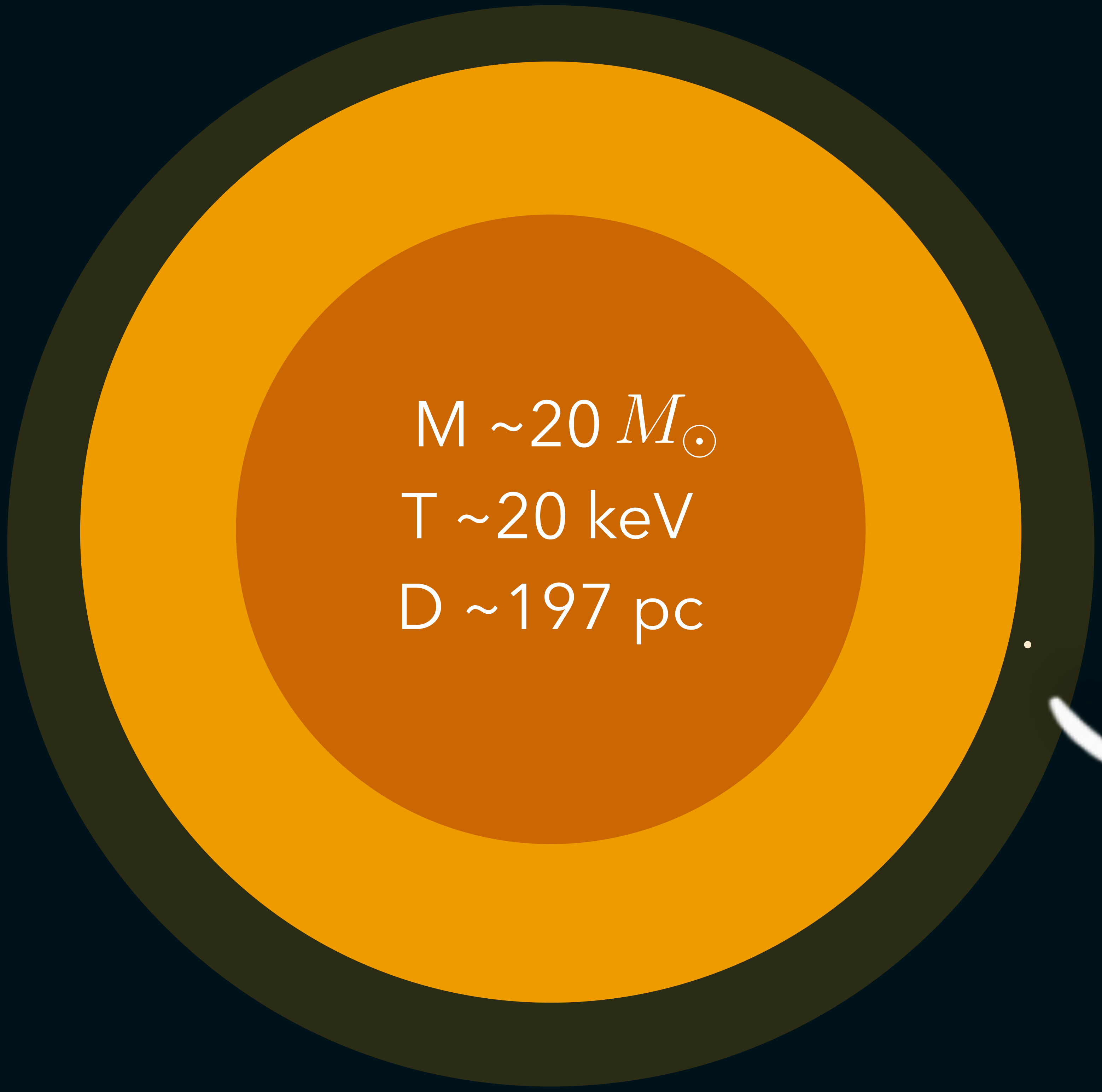

Magnetic dipole (M1) Nuclear transition

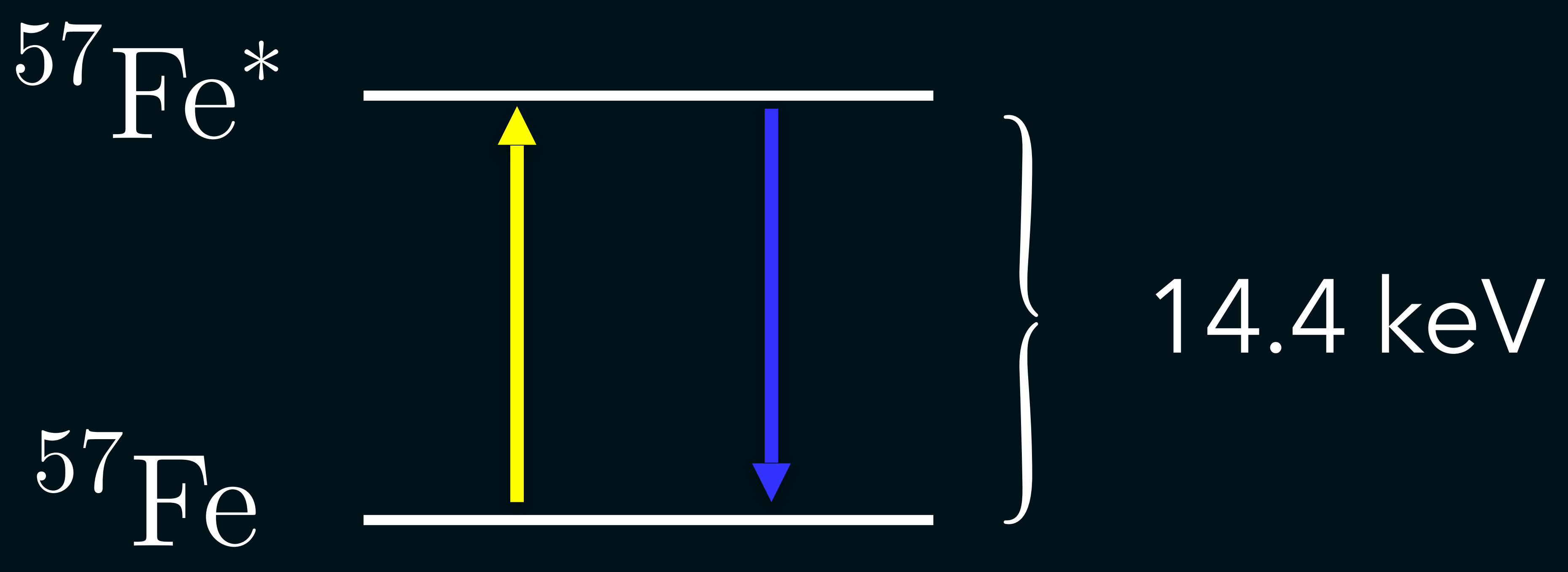

$$\frac{\Gamma_a}{\Gamma_\gamma} = 2.32\,\underbrace{(0.16 g_{ap} + 1.16 g_{an})}_{g_{aN}^{\mathrm{eff}}}$$

FRC, P. Casaseca, M. Giannotti, M. Kaltschmidt, J. Ruz, J. K. Vogel
Phys.Rev.D *112 (2025) 12, 12*

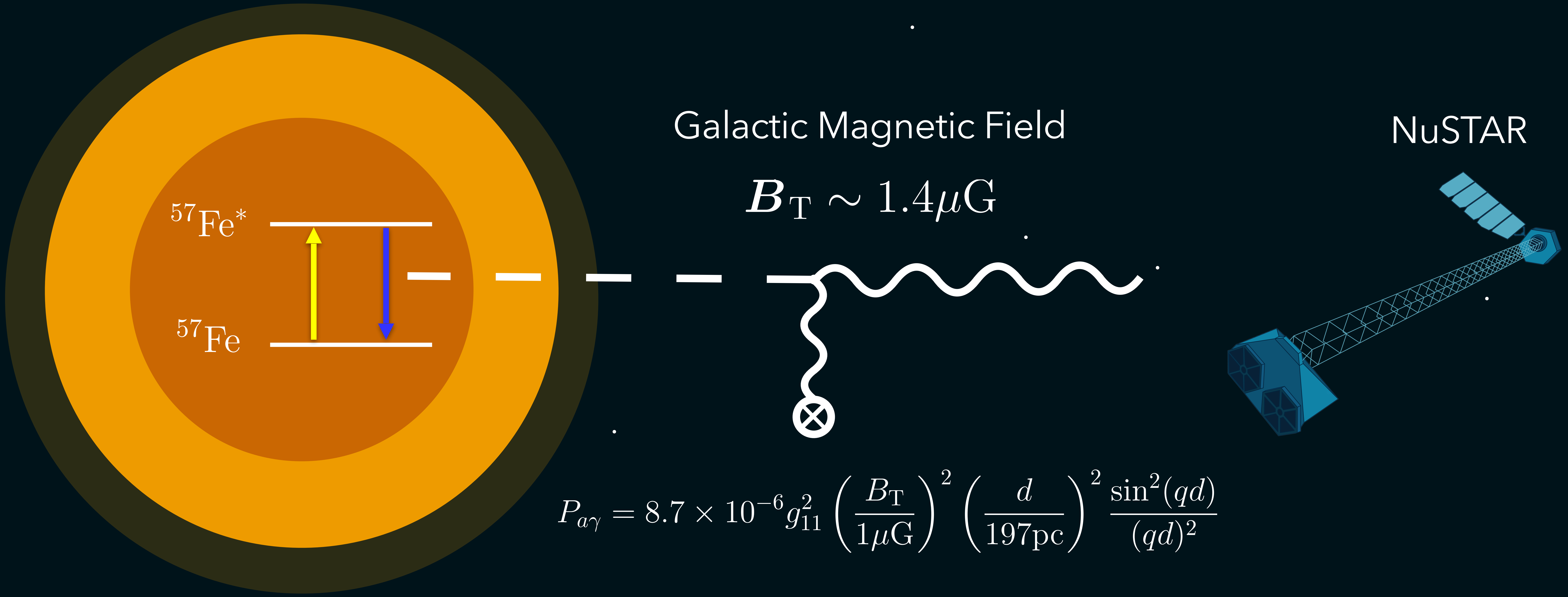

$$P_{a\gamma} = 8.7 \times 10^{-6} g_{11}^2 \left(\frac{B_{\mathrm{T}}}{1\mu\mathrm{G}}\right)^2 \left(\frac{d}{197\mathrm{pc}}\right)^2 \frac{\sin^2(qd)}{(qd)^2}$$

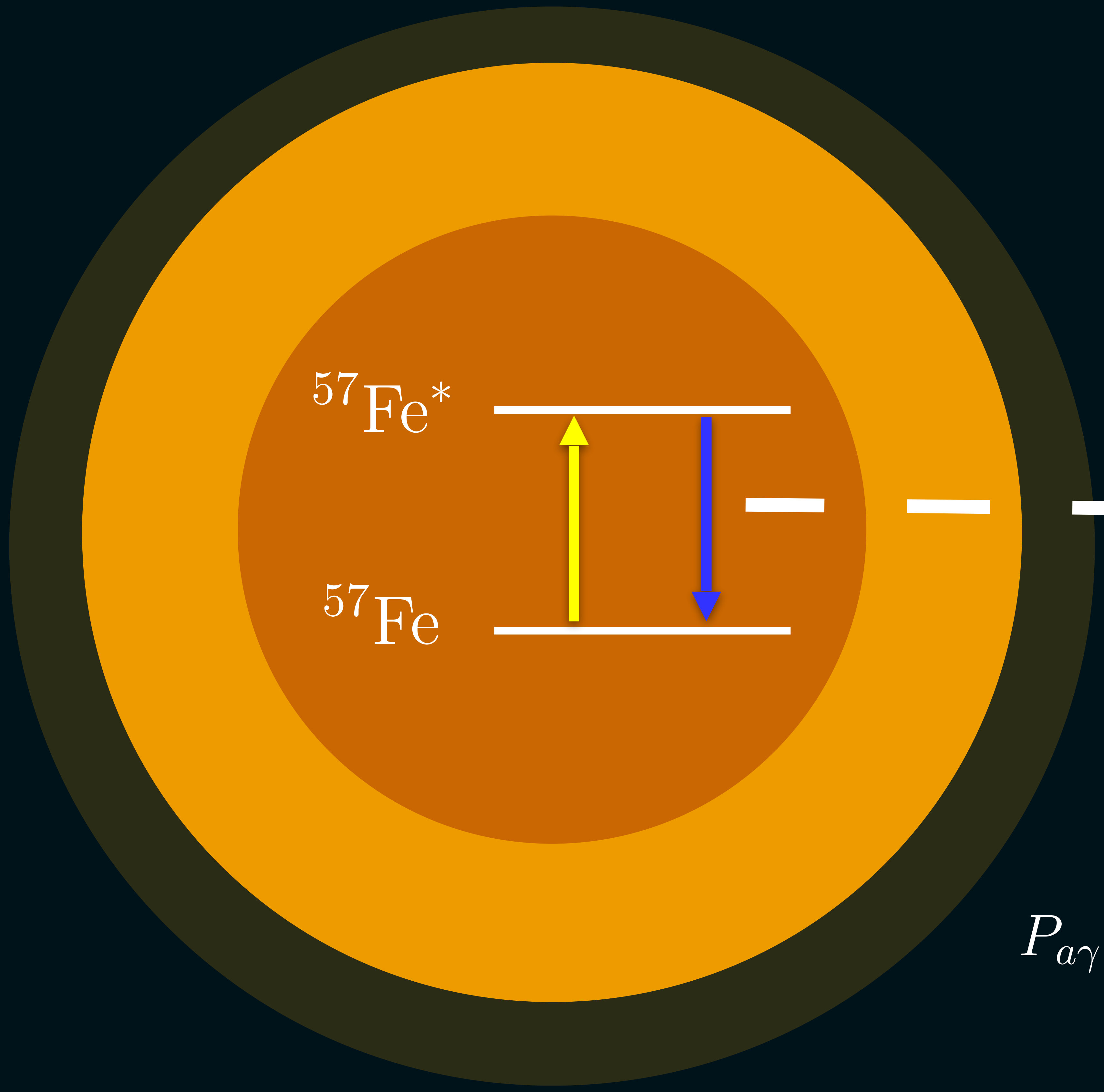

Galactic Magnetic Field

$$\boldsymbol{B}_\mathrm{T} \sim 1.4\mu\mathrm{G}$$

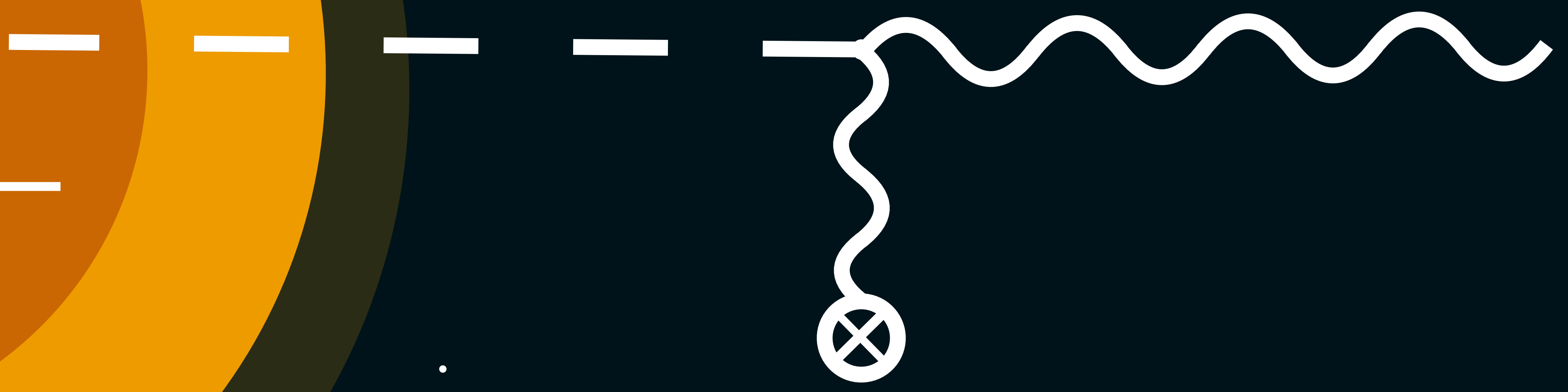

NuSTAR

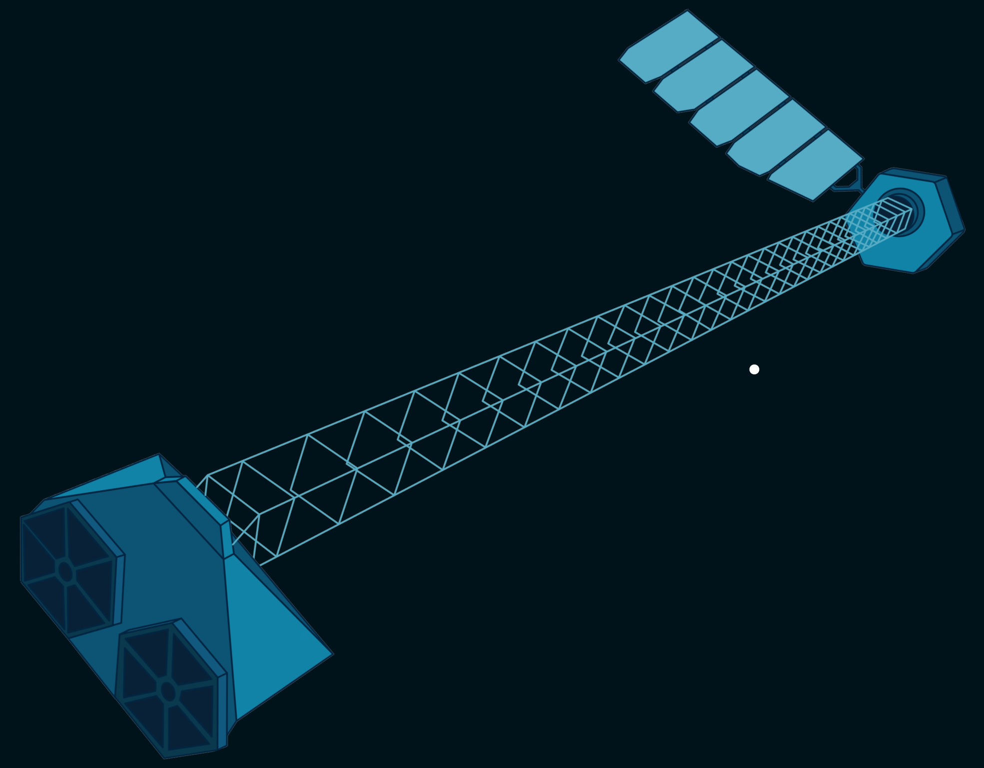

$$P_{a\gamma} = 8.7 \times 10^{-6} g_{11}^2 \left(\frac{B_\mathrm{T}}{1\mu\mathrm{G}}\right)^2 \left(\frac{d}{197\mathrm{pc}}\right)^2 \frac{\sin^2(qd)}{(qd)^2}$$

1

1. Stelar simulations
2. Theoretical axion flux.

2

3. B field and conversion.
4. Axion induced photon flux at NuSTAR

3

5. Observational data
6. Unbinned likelihood analysis.

Stellar simulations

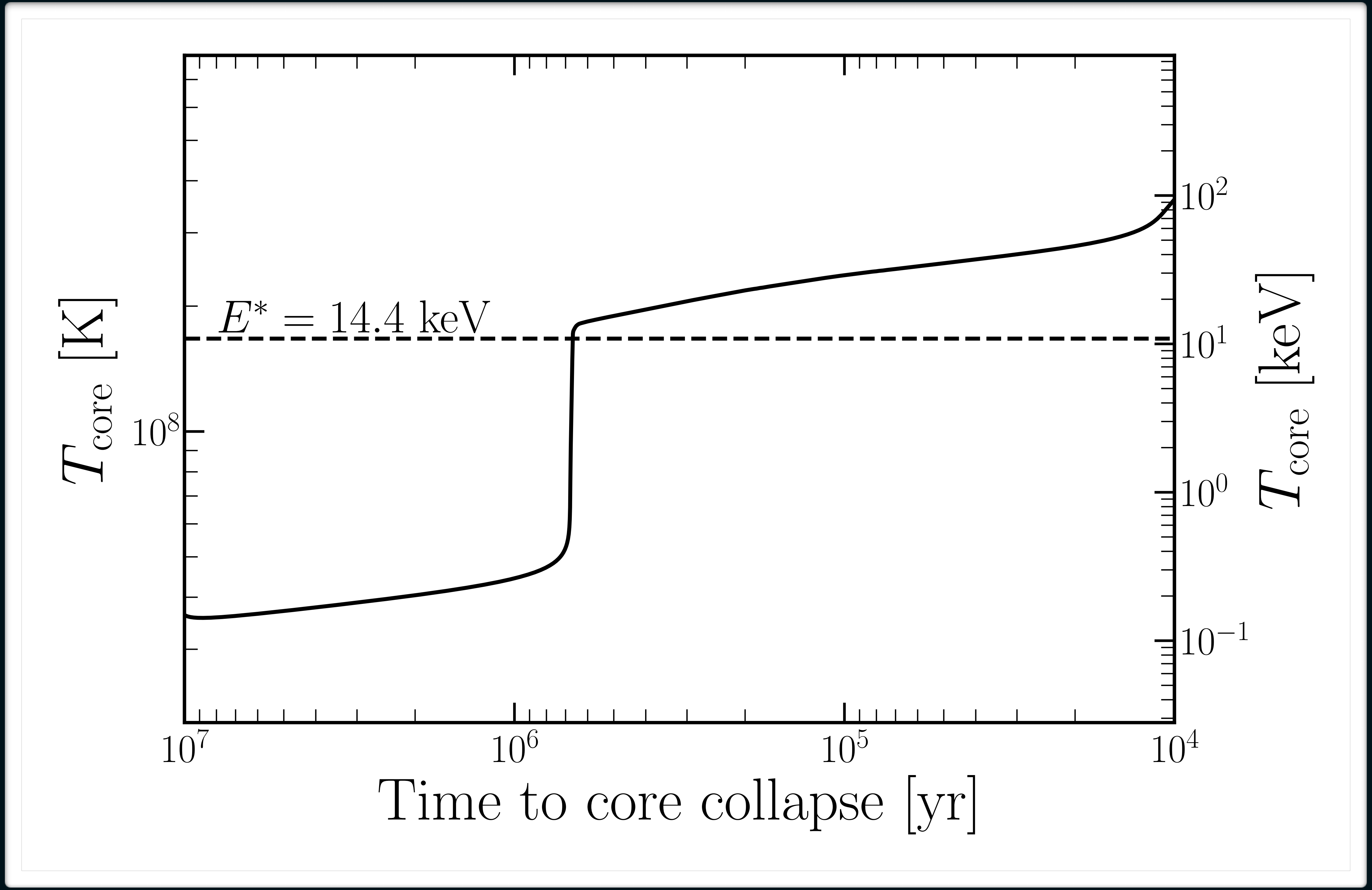

MESA

Modules for Experiments in **Stellar Astrophysics**

Stellar simulations

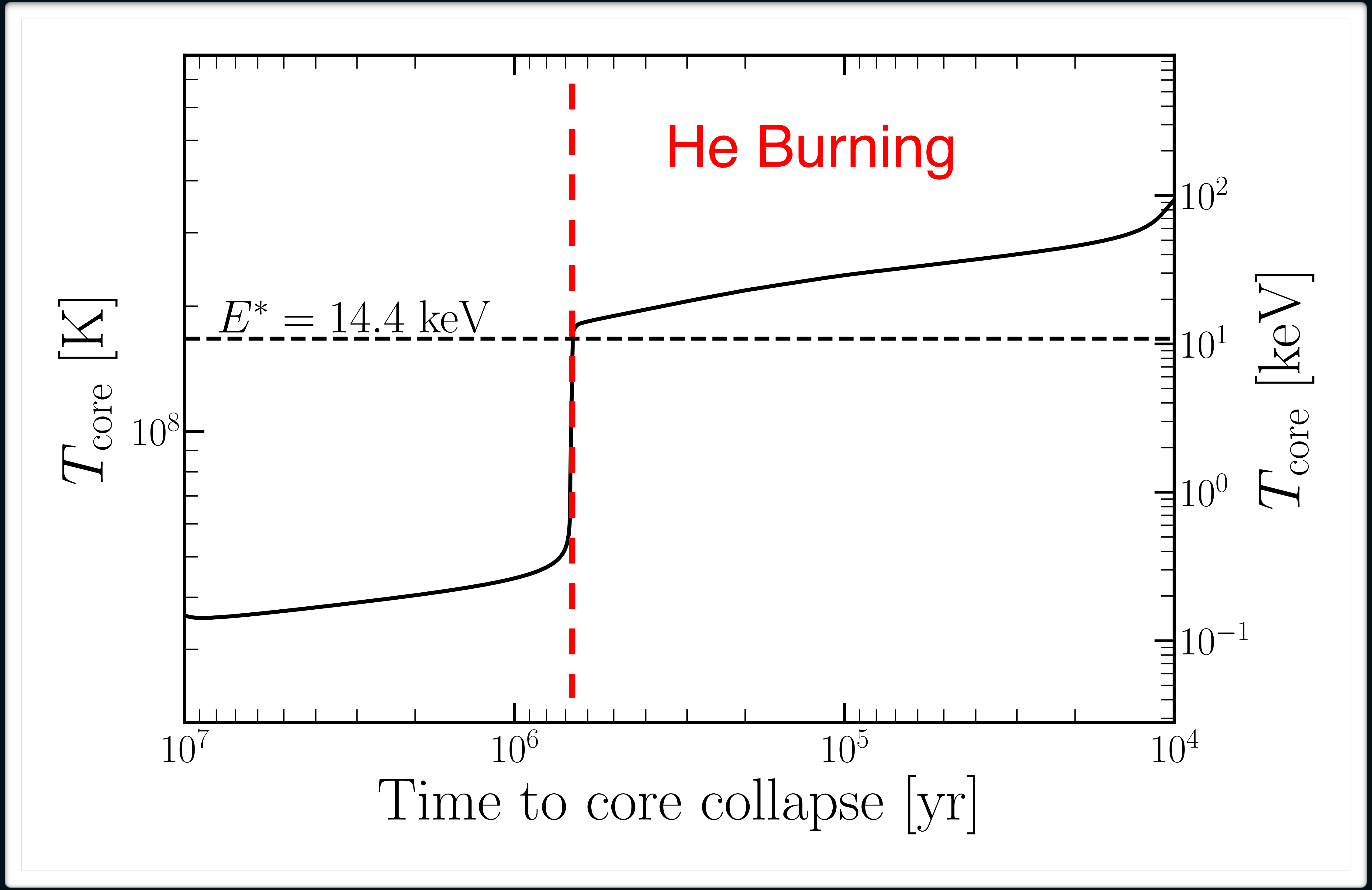

MESA

Modules for Experiments in **Stellar Astrophysics**

Stellar simulations

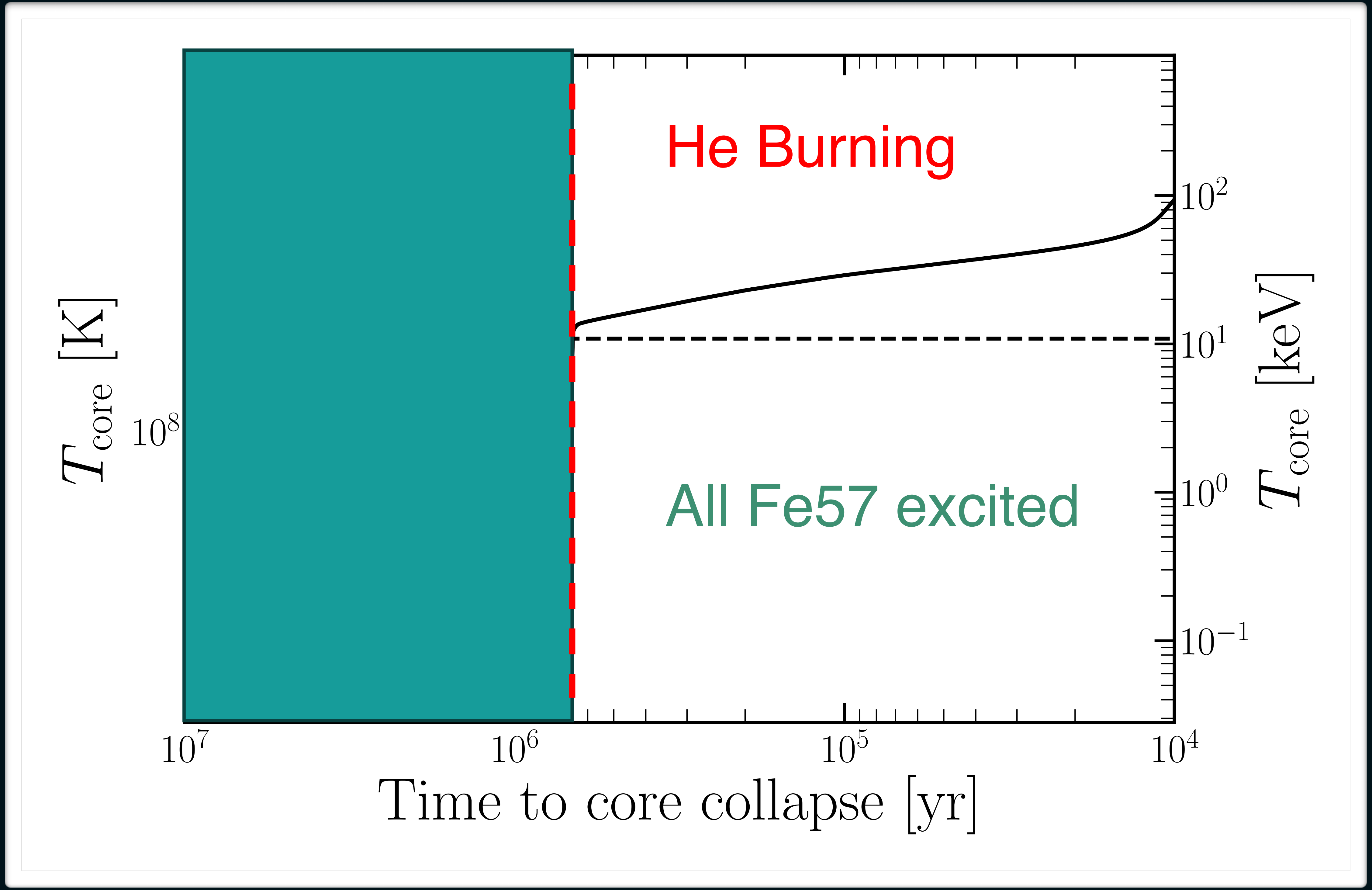

MESA

Modules for Experiments in **Stellar Astrophysics**

Observed NuSTAR spectra

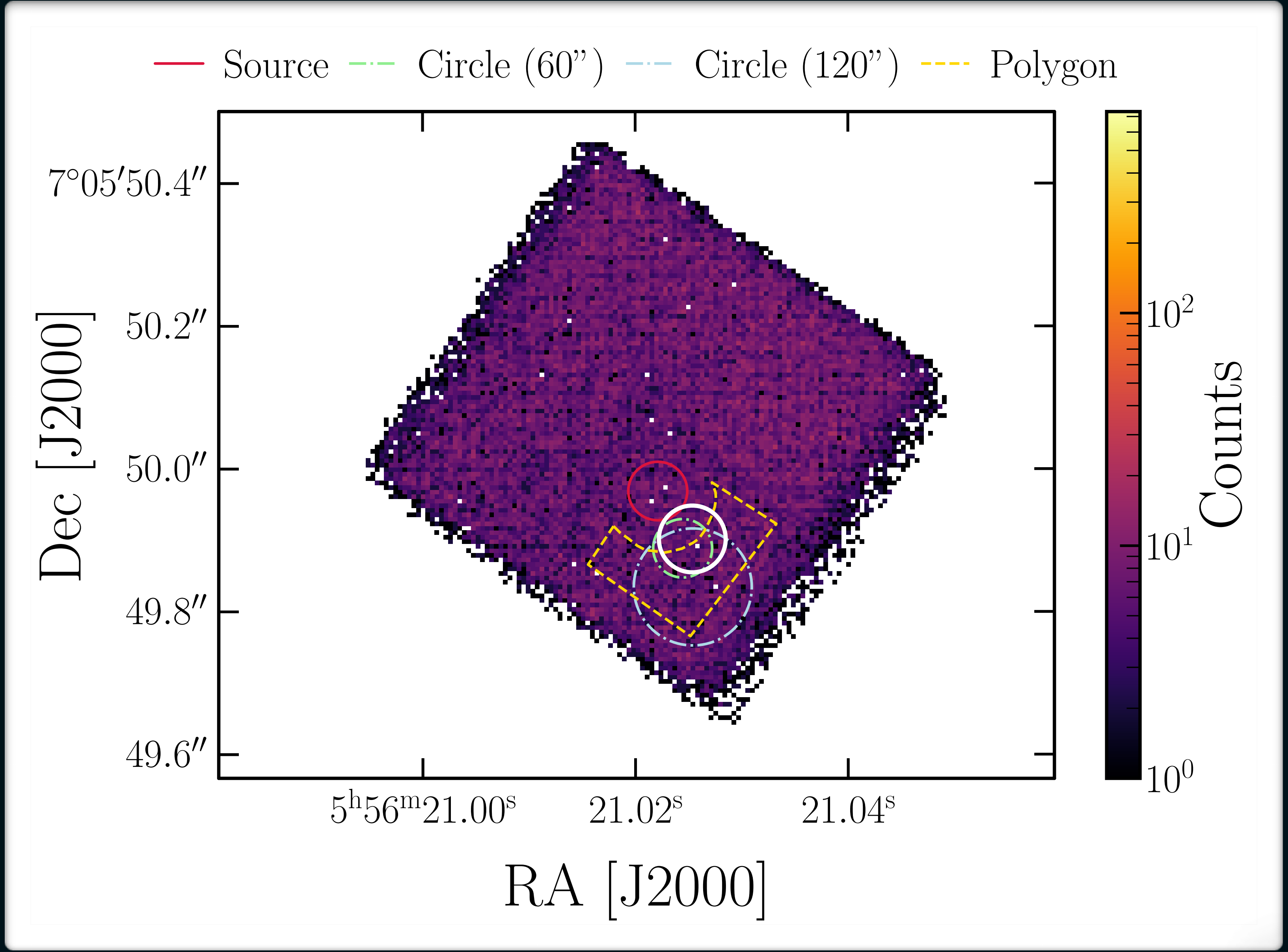

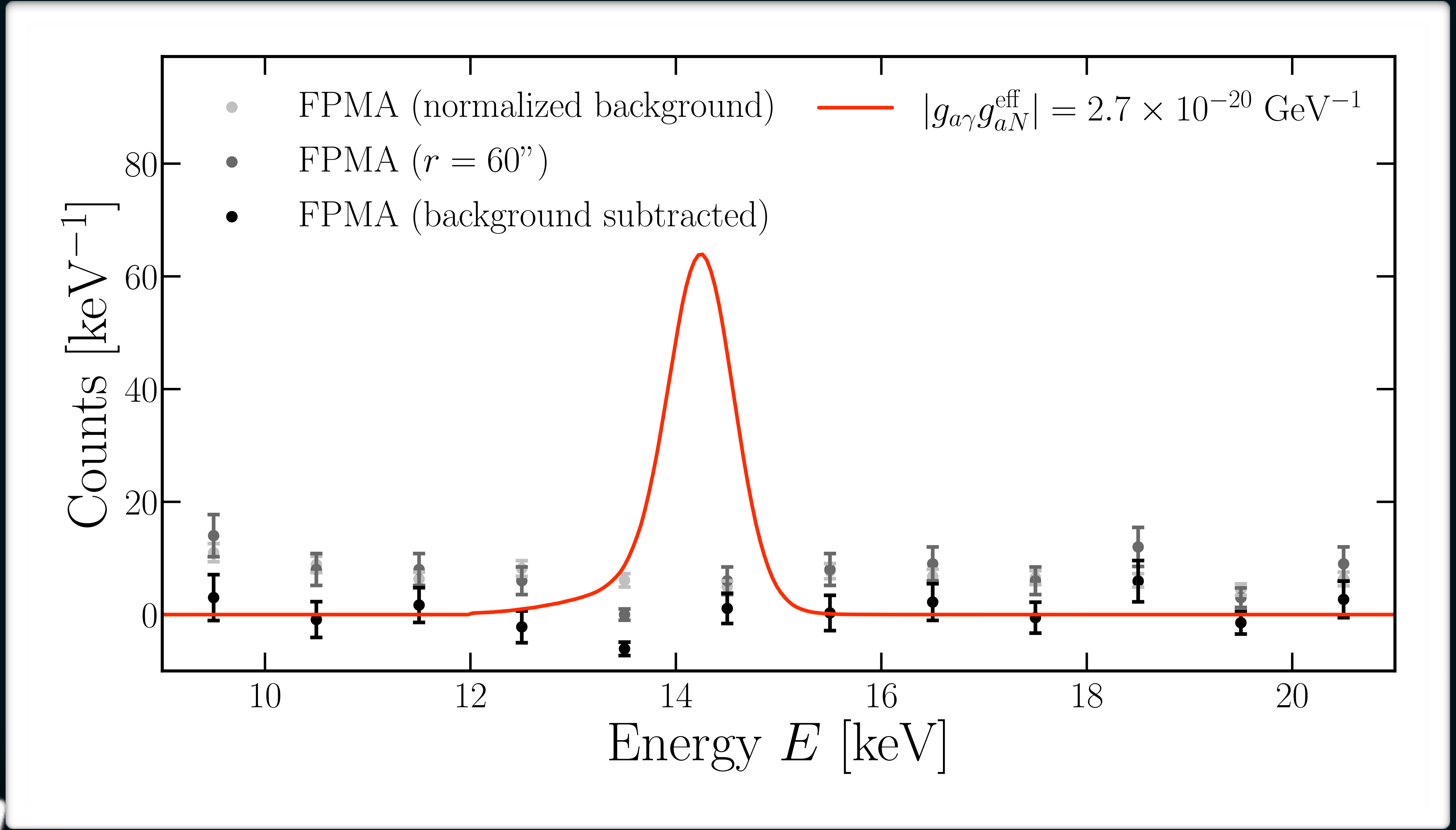

NASA data analysis tools: HEASOFT, NuSTARdas, XSPEC

Betelgeuse constraints

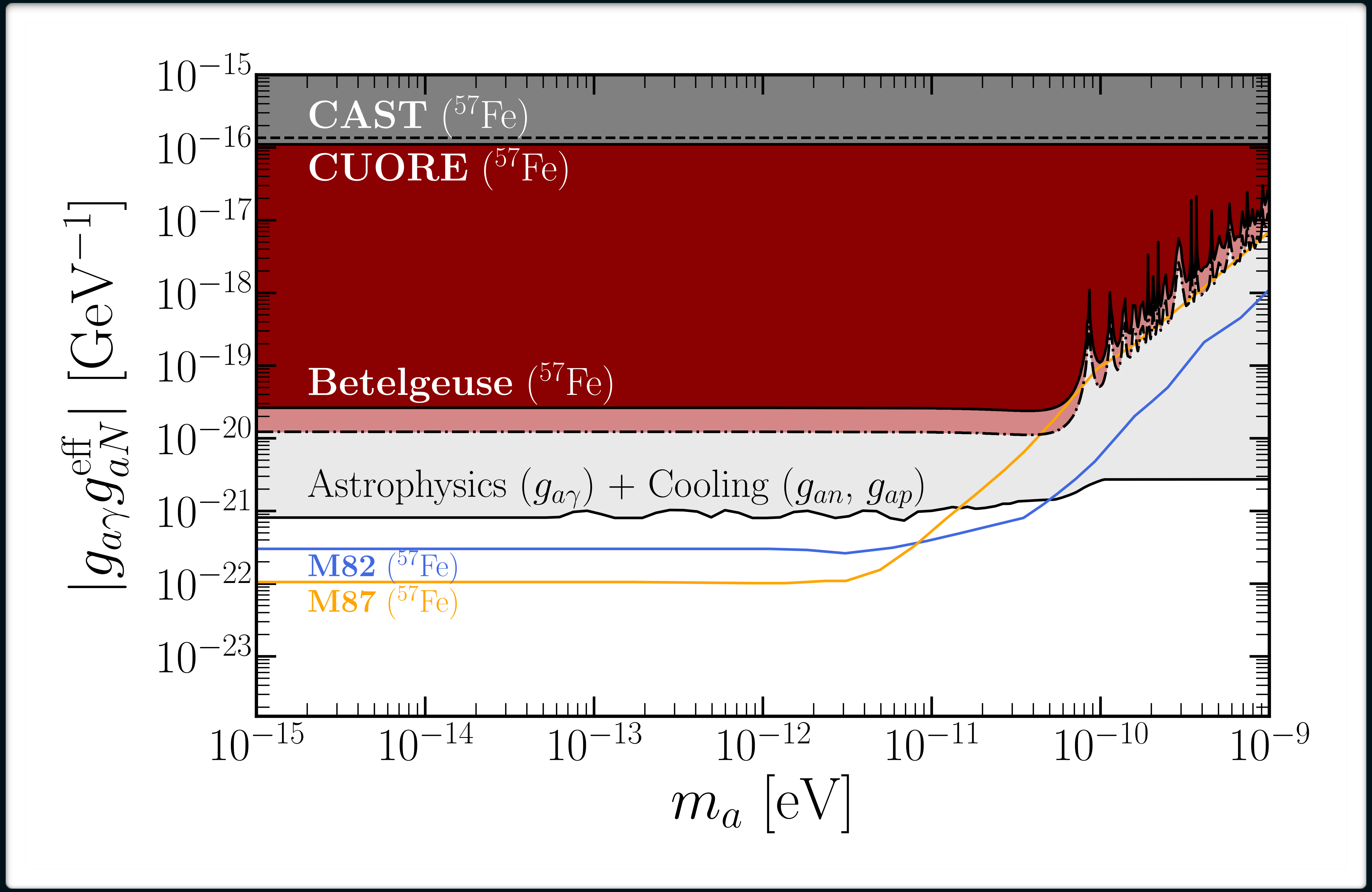

Betelgeuse constraints

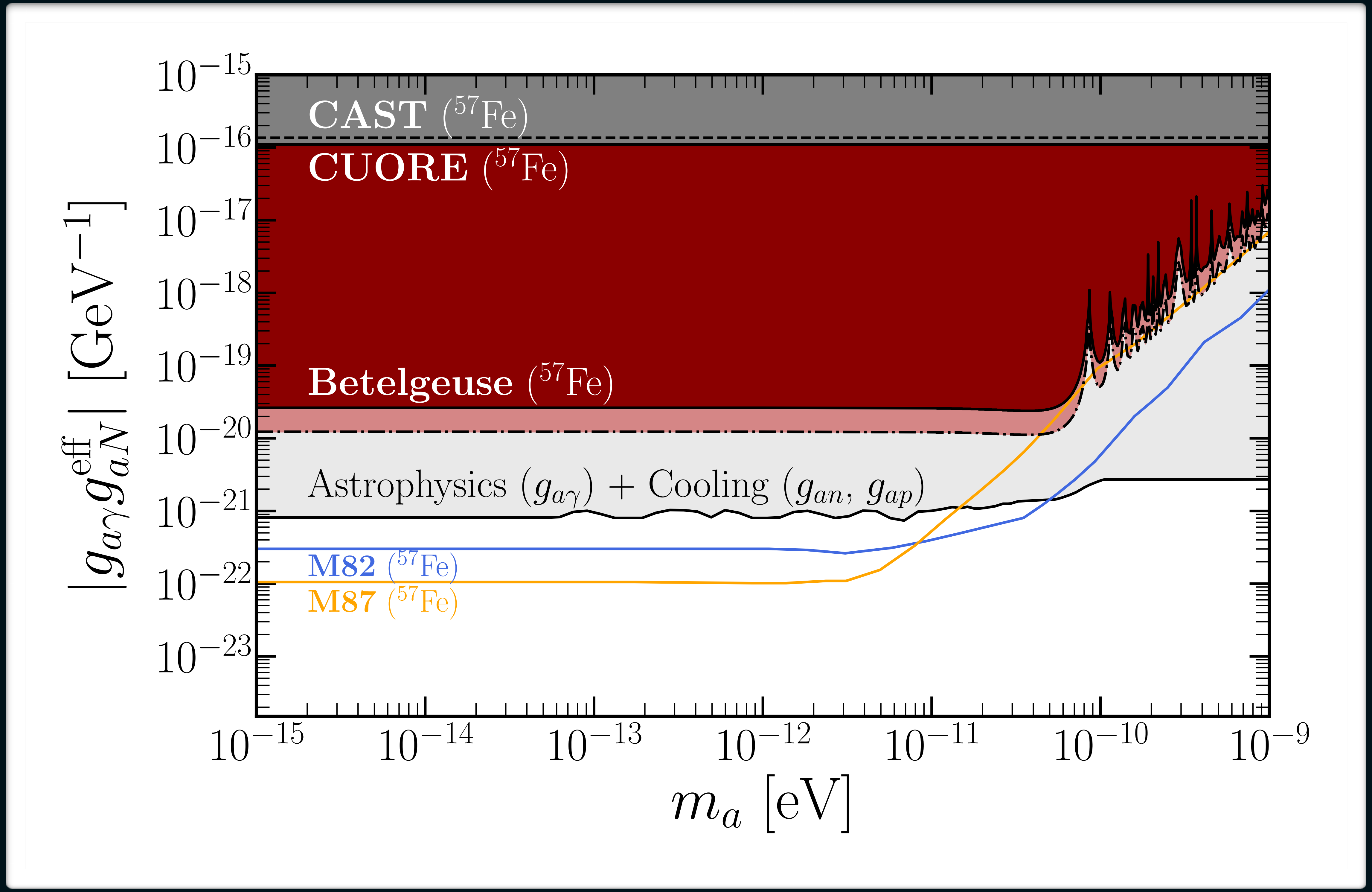

FRC, P. Casaseca, M. Giannotti, M. Kaltschmidt, J. Ruz, J. K. Vogel
Phys.Rev.D *112 (2025) 12, 12*

The M82 case

- M82 is a **starburst galaxy** at 3.8 Mpc.
- Heavy Axion emission dominated by **young massive stars.**

$$N_{\rm tot} = 1.8 \times 10^{10}$$

The M82 case

Production in the individual stars of M82 via:

Primakoff Conversion

$$\gamma + Ze \to a + Ze$$

Photon Coalescence

$$\gamma + \gamma \longrightarrow a$$

- M82 is a **starburst galaxy** at 3.8 Mpc.
- Heavy Axion emission dominated by **young massive stars.**

$$N_{\rm tot} = 1.8 \times 10^{10}$$

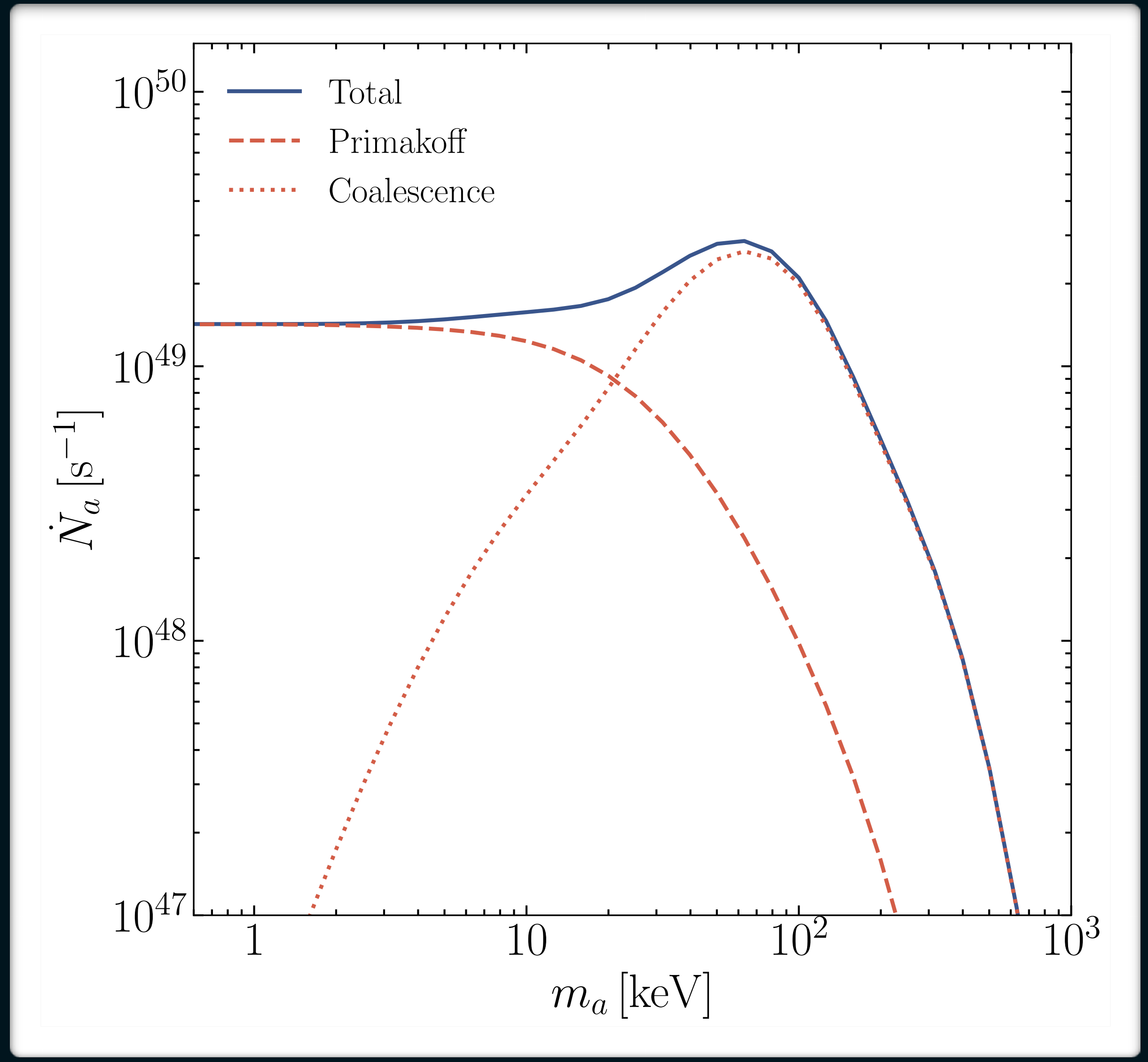

Heavy ALPs **Decay**

$m_a \sim 30 - 500\text{keV}$

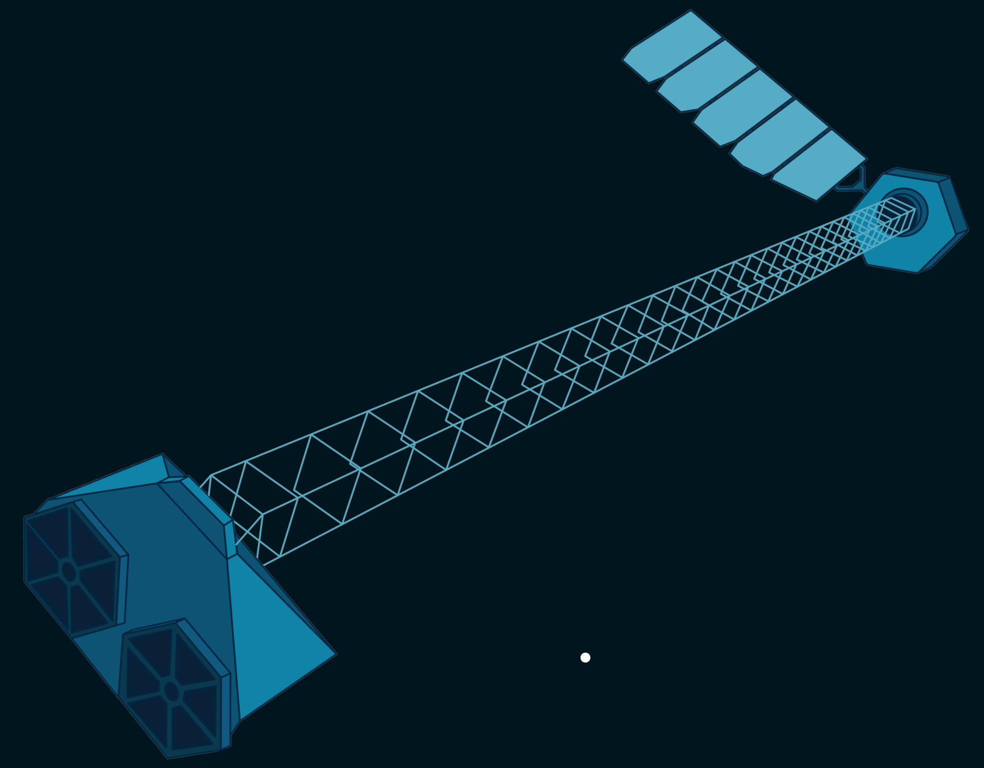

Heavy ALPs **Decay**

$m_a \sim 30 - 500\mathrm{keV}$

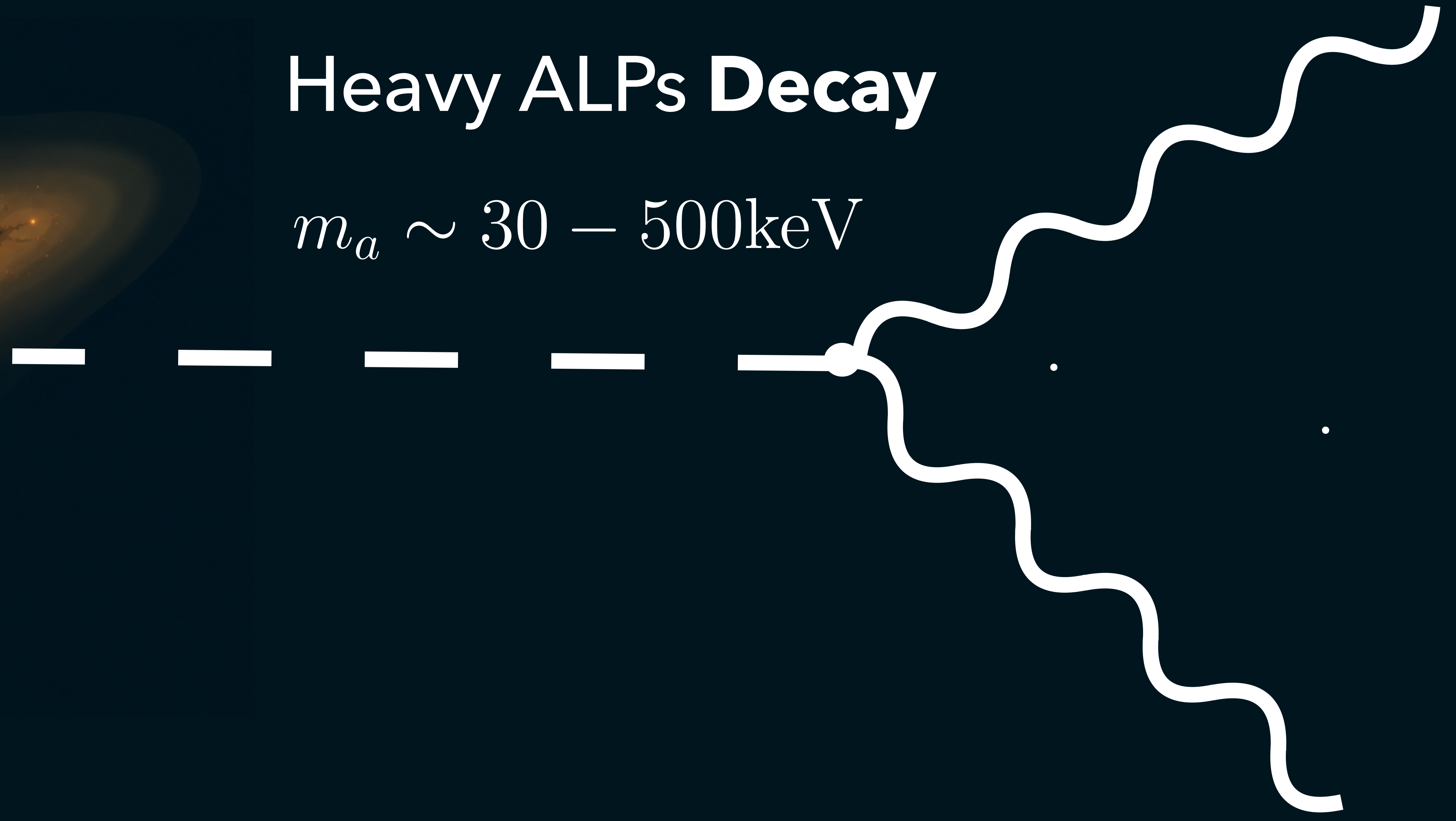

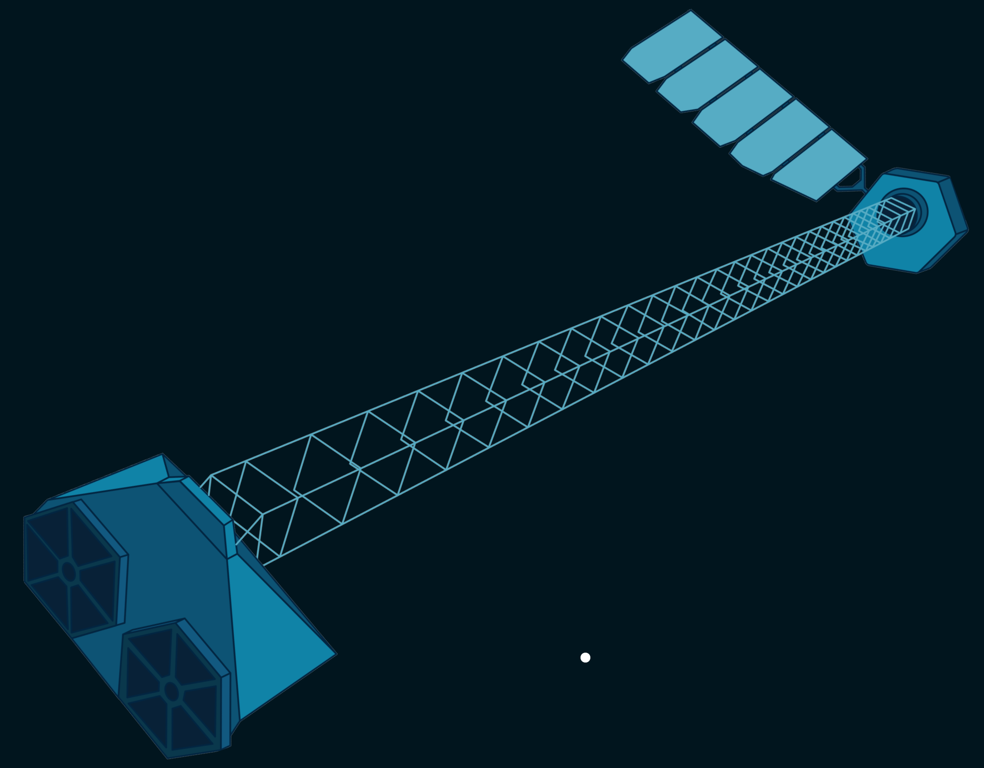

Total Axion Flux

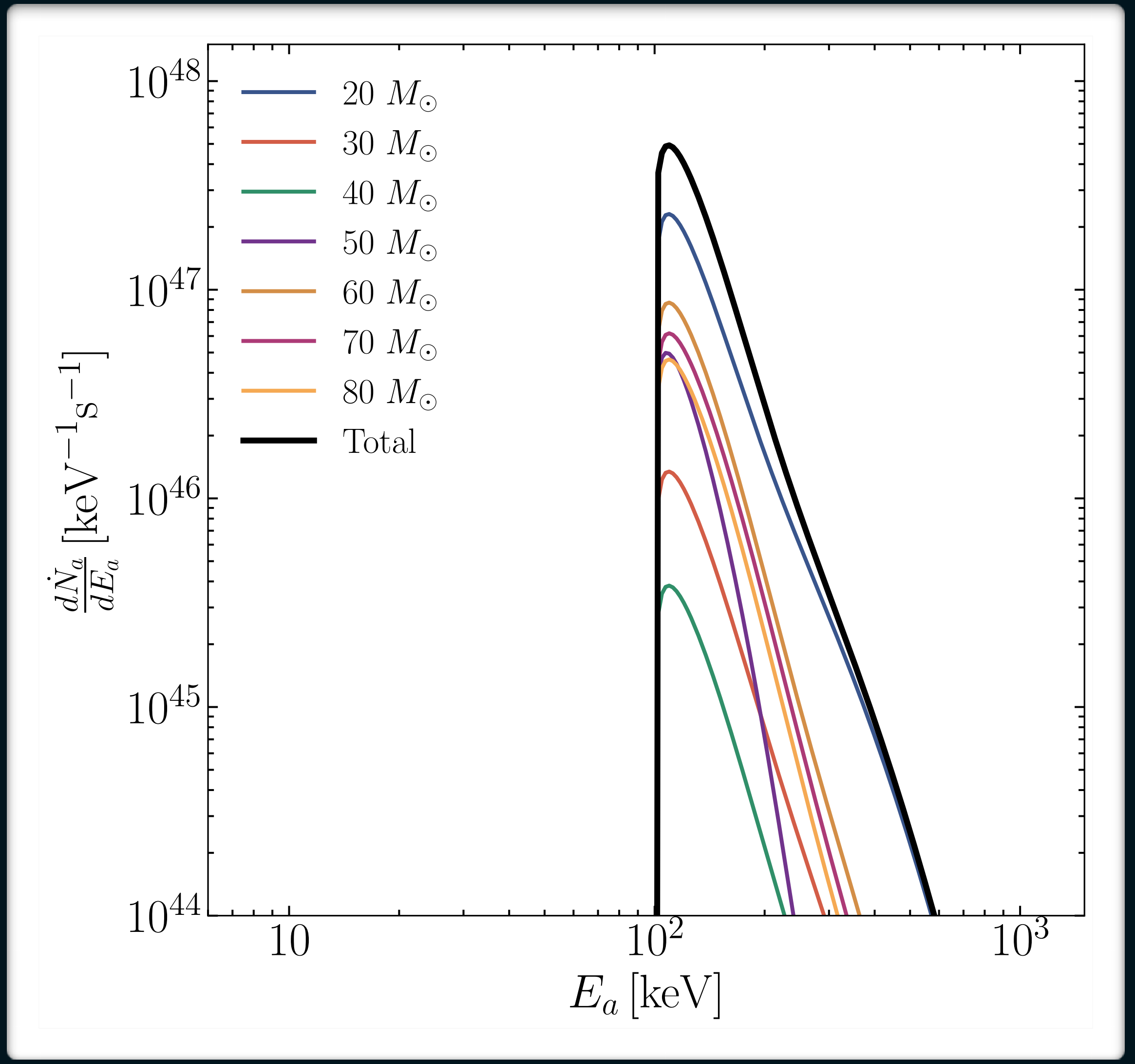

$$\frac{dN_a}{dE_a} = N_{\rm tot} \int dM_s dt_s \, \mathrm{IMF}\,(M_s)\, \mathrm{SFH}\,(t_s)\, \frac{dN_a^s}{dE_a}$$

The axion-photon flux

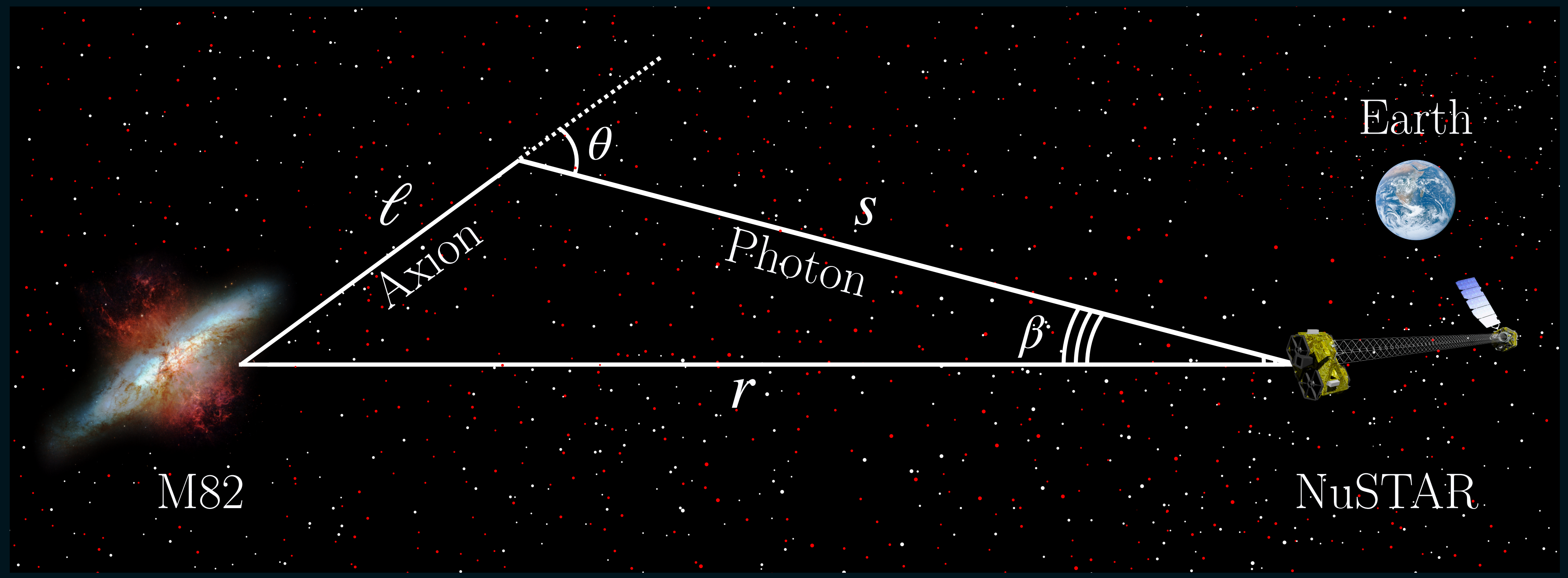

$$\frac{d\Phi_\gamma}{dE_\gamma d\beta} = \int_{E_{a,\min}}^{+\infty} \frac{2dE_a \cos\beta}{p_a} \frac{d\dot{N}_a/dE_a}{4\pi r} \Theta(\cos\beta - \cos\theta) \exp\left[-\frac{\Gamma_a m_a r \sin\beta}{p_a \sin\theta}\right] \frac{\Gamma_a m_a}{p_a \sin\theta}$$

$$\Gamma_a = g_{a\gamma}^2 m_a^3 / 64\pi$$

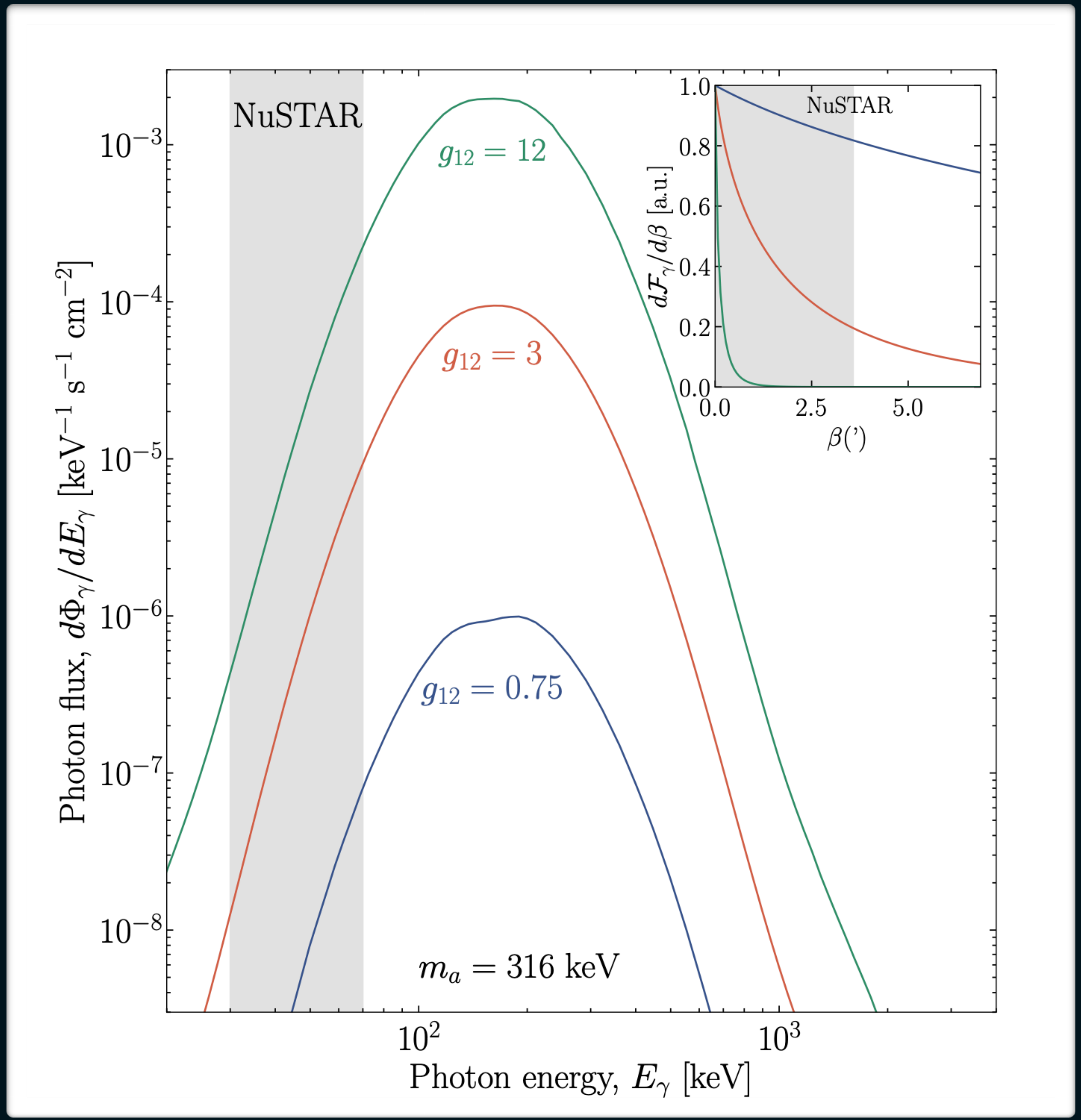

M82 axion decay constraints

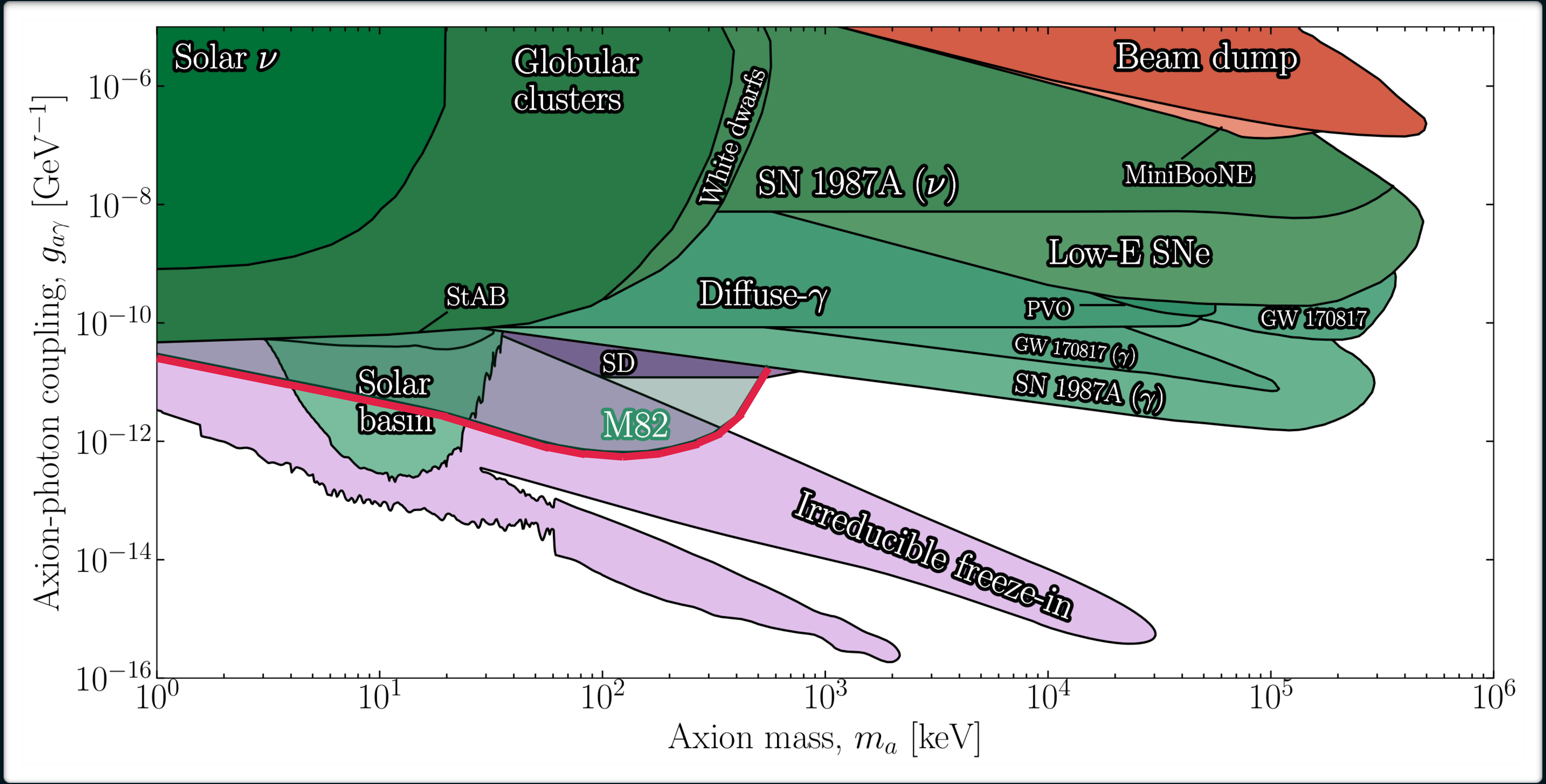

FRC, D.F.G. Fiorillo, G.L. Lucente, E. Vitagliano, J.Vogel
Physical Review Letters, 134.171004

Overview

14.4 keV excited state of Fe57 in nearby **RSG** provides a stable, narrow line-like axion X-ray signature.

The decay of slow axions from **starburst Galaxies** leads the strongest constraints for masses between 30 MeV - 500 MeV .

X-ray Telescopes like NuSTAR, Chandra, and **future missions** like Athena and HEX-P, are key in the quest of axions.

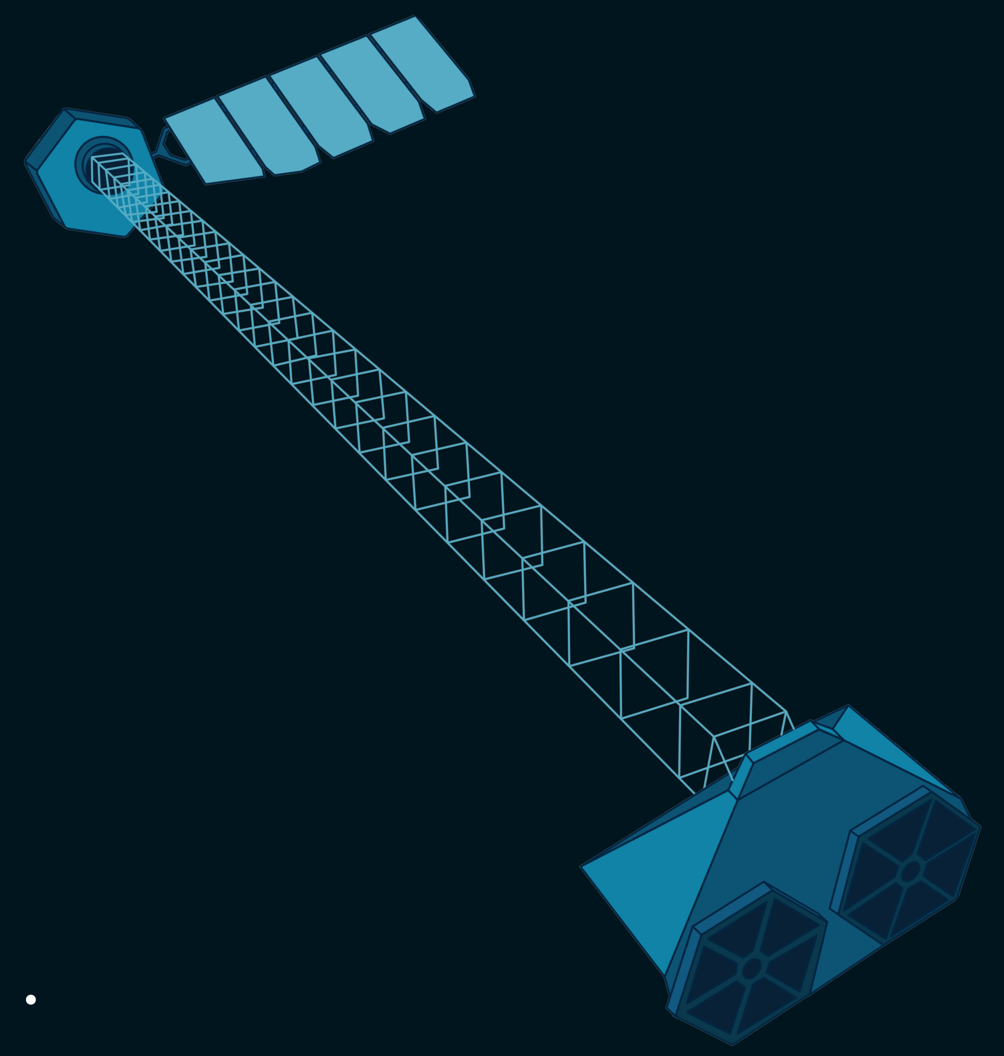

Probability conversion

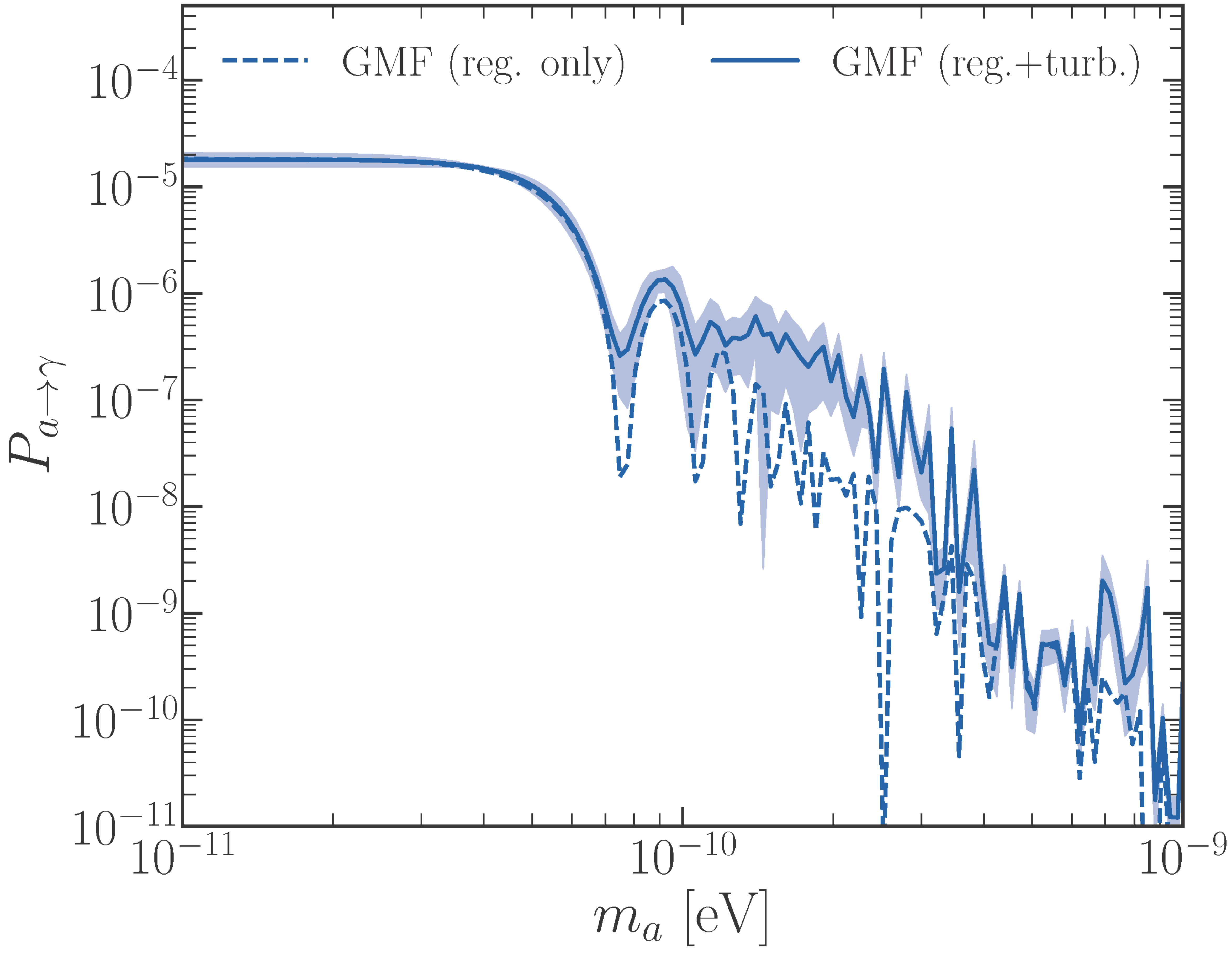

Galactic Magnetic Field

Regular + Turbulent

$$P_{a\gamma} = 8.7 \times 10^{-6} g_{11}^2 \left(\frac{B_\mathrm{T}}{1\mu\mathrm{G}}\right)^2 \left(\frac{d}{197\mathrm{pc}}\right)^2 \frac{\sin^2(qd)}{(qd)^2}$$

$$g_{11} = \left(g_{a\gamma}/10^{11}\mathrm{GeV}^{-1}\right)$$

Axion flux

$$\frac{\mathrm{d}N_a(E)}{\mathrm{d}E} = \frac{1}{4\pi d^2}\int_0^{R_{\mathrm{star}}} \mathcal{N}_a(r)\mathcal{G}(E,\sigma(r))\rho(r)4\pi r^2$$

Where $\mathcal{N}_a$ is the axion rate that depends on the Fe57 number density, the occupation of the first excited state and the branching factor ratio

$$\frac{\Gamma_a}{\Gamma_\gamma} = 2.32\left(\underbrace{0.16 g_{ap} + 1.16 g_{an}}_{g_{aN}^{\mathrm{eff}}}\right)^2$$

Axion flux

$$\frac{d\Phi_\gamma}{dE_\gamma d\beta} = \int_{E_{a,\min}}^{+\infty} \frac{2dE_a \cos\beta}{p_a} \frac{d\dot{N}_a/dE_a}{4\pi r}$$
$$\Theta(\cos\beta - \cos\theta) \exp\left[-\frac{\Gamma_a m_a r \sin\beta}{p_a \sin\theta}\right] \frac{\Gamma_a m_a}{p_a \sin\theta}$$

$$\cos\theta = \frac{1}{v_a}\left[1 - \frac{E_a}{2E_\gamma}(1 - v_a^2)\right]$$

$$\Gamma_a = g_{a\gamma}^2 m_a^3 / 64\pi$$

Likelihood analysis

Unbinned likelihood $$\mathcal{L} = \prod_{i=\{\mathrm{A,B}\}} \mathcal{L}_i \times \prod_{i=\{\mathrm{A,B}\}} \mathcal{G}\left(\delta^i_{\mathrm{bkg}} \sigma^i_{\mathrm{bkg}}\right)$$

$$\begin{aligned}\mathcal{L}_i &= \mathrm{Poisson}\left(N_{\mathrm{obs},i} \mid N_{\mathrm{exp},i}\right) \\ &\times \prod_{j=1}^{N_{\mathrm{obm},i}} \left[\frac{N_{\mathrm{ax},i} P_{\mathrm{ax}}\left(E'_j\right)}{N_{\mathrm{cxp},i}} + \frac{N_{\mathrm{bkg},i}\left(1+\delta^i_{\mathrm{bkg}}\right) P_{\mathrm{bkg}}\left(E'_j\right)}{N_{\mathrm{exp},i}}\right]\end{aligned}$$

$$P(\theta) = \frac{\mathcal{L}(\theta)}{\int \mathcal{L}\left(\theta'\right) \mathrm{d}\theta'} \qquad \int_0^{\left(g^2_{a\gamma} g^2_{aN}\right)_{as\%}} P\left(g^2_{a\gamma} g^2_{aN}\right) \mathrm{d}\left(g^2_{a\gamma} g^2_{aN}\right) = 0.95$$

M82 FOV

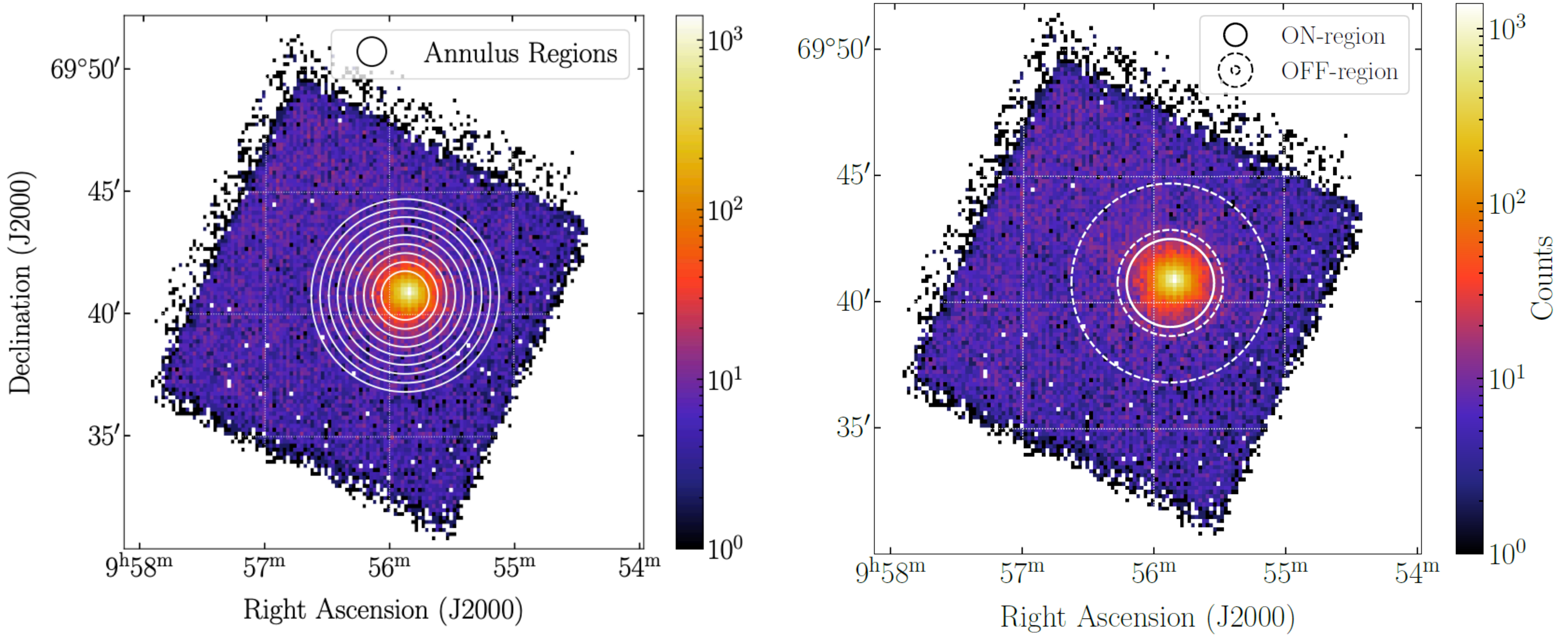

$$N^a_{c,i,\alpha}\left(g_{a\gamma}, m_a\right) = t^c \int dE' \,\mathrm{RMF}^c_{i,\alpha}\left(E_i, E'\right) \mathrm{ARF}^c_\alpha\left(E'\right) S_\alpha\left(E' \mid g_{a\gamma}, m_a\right)$$

M82 FOV

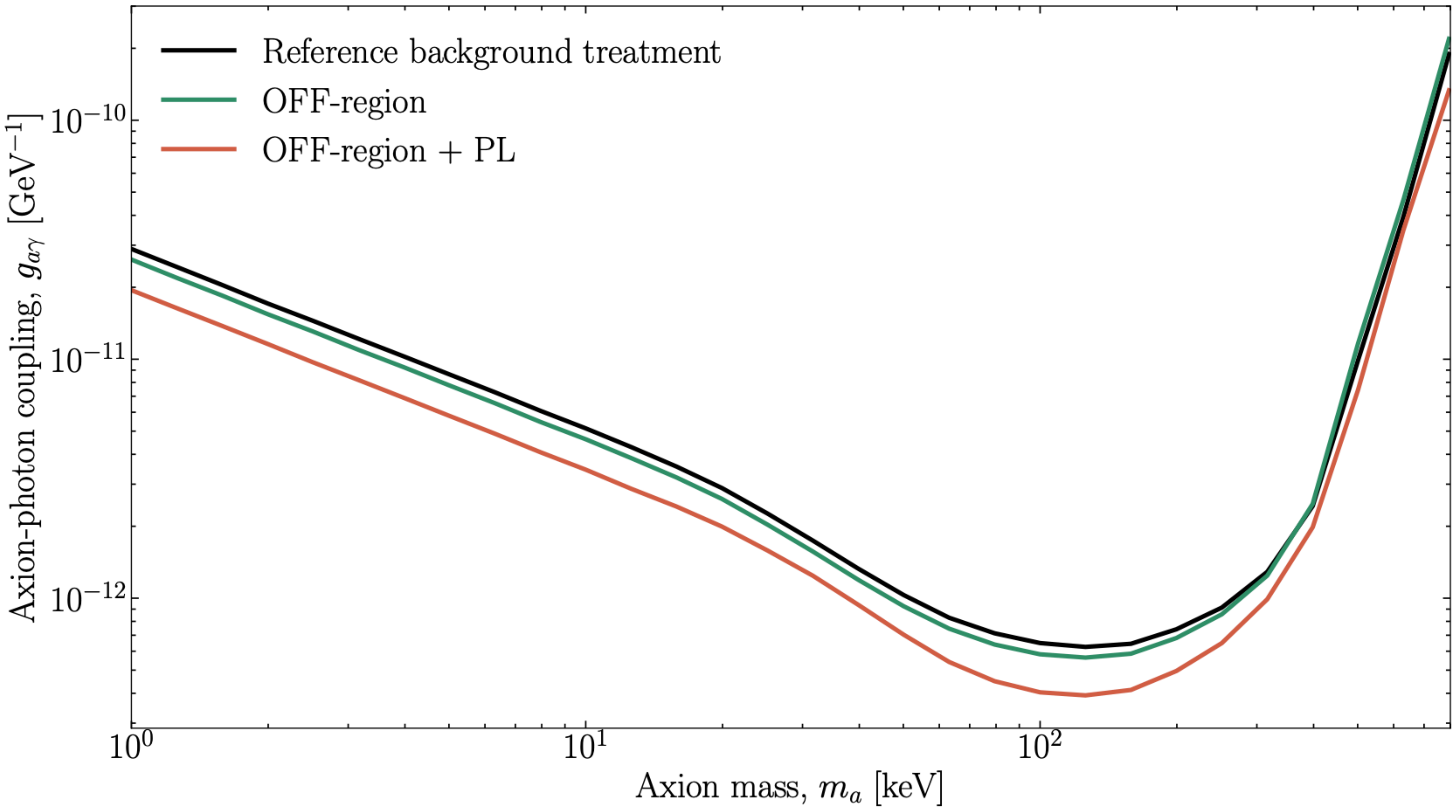

Reference background treatment
OFF-region
OFF-region + PL
Axion-photon coupling, $g_{a\gamma}$ [GeV^{-1}]
10^{-10}
10^{-11}
10^{-12}
10^{0}
10^{1}
10^{2}
Axion mass, m_a [keV]

M82 Spectra

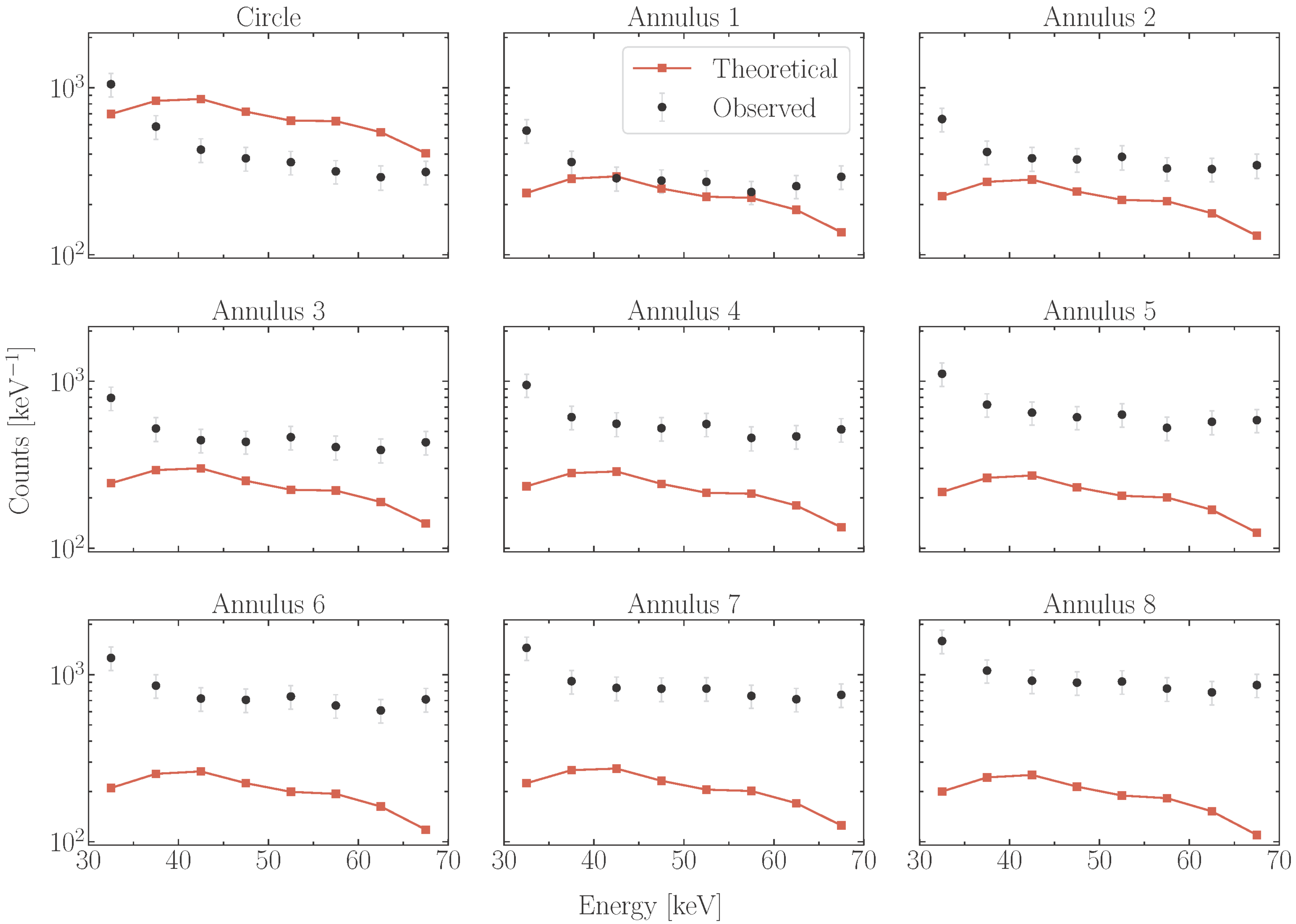

Circle
Annulus 1
Annulus 2
Annulus 3
Annulus 4
Annulus 5
Annulus 6
Annulus 7
Annulus 8
Theoretical
Observed
10^3
10^2
Counts [keV^{-1}]
30
40
50
60
70
Energy [keV]

NuSTAR as Axion Helioscope

1 Production due to the electric fields in the core

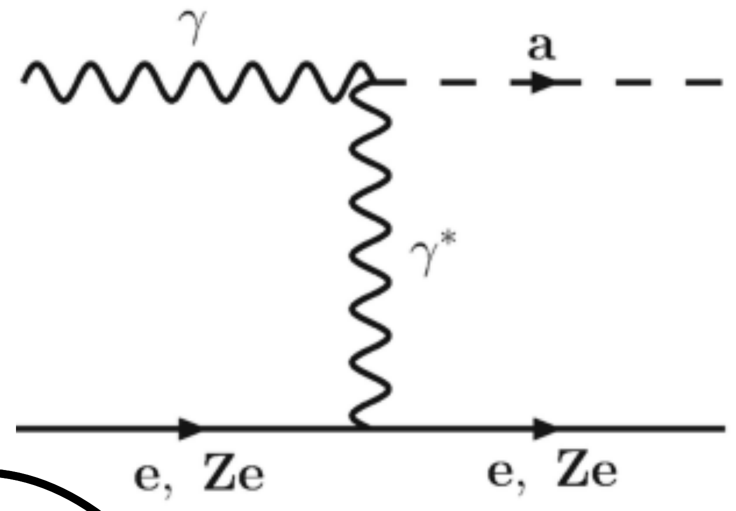

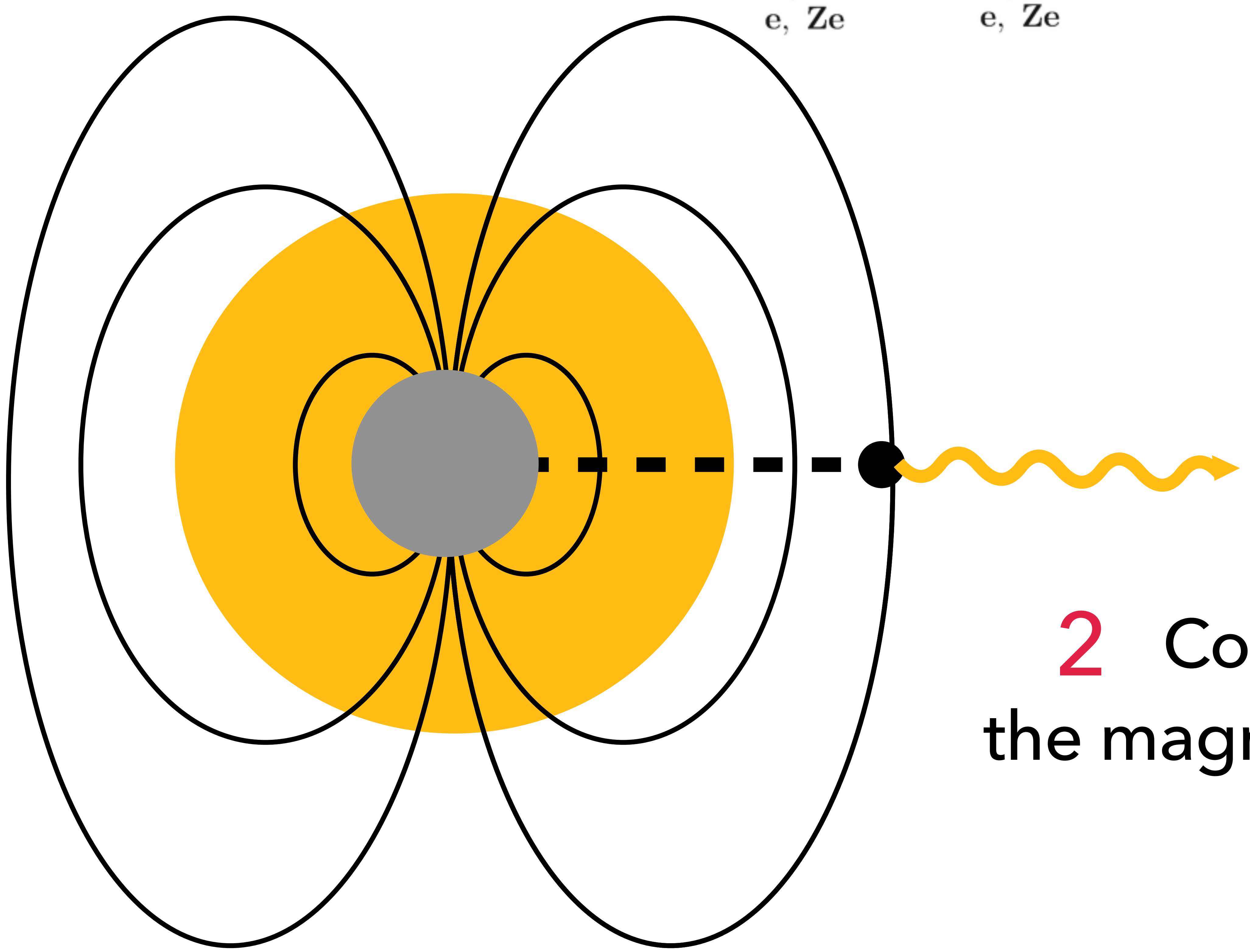

2 Conversion in the magnetic solar B field

3 X-ray detection With NuSTAR

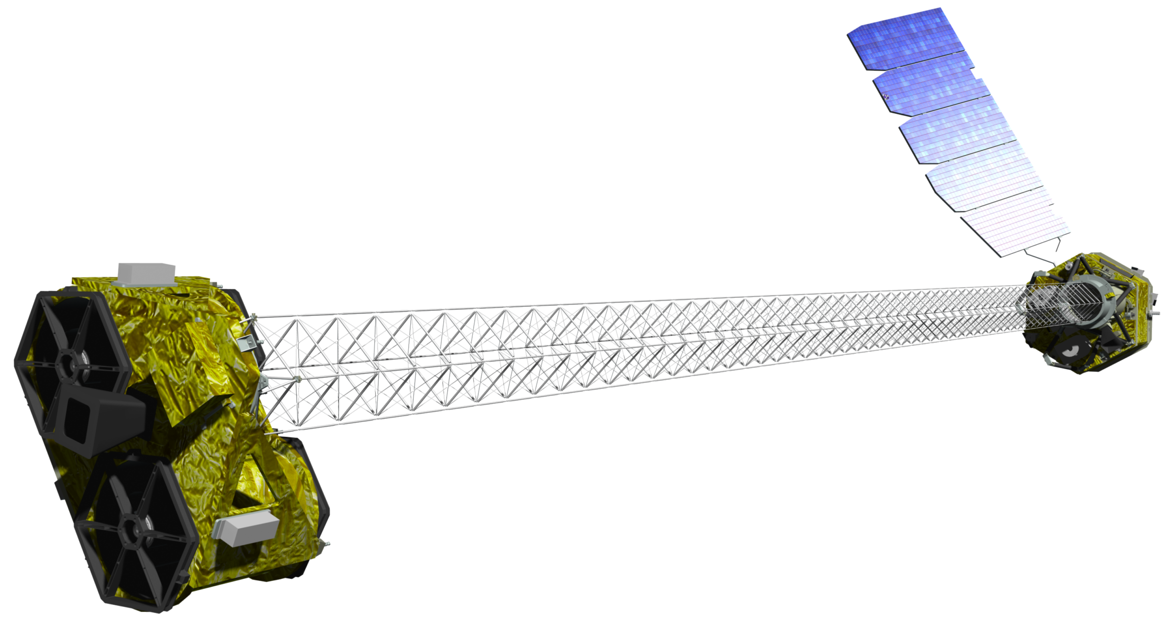

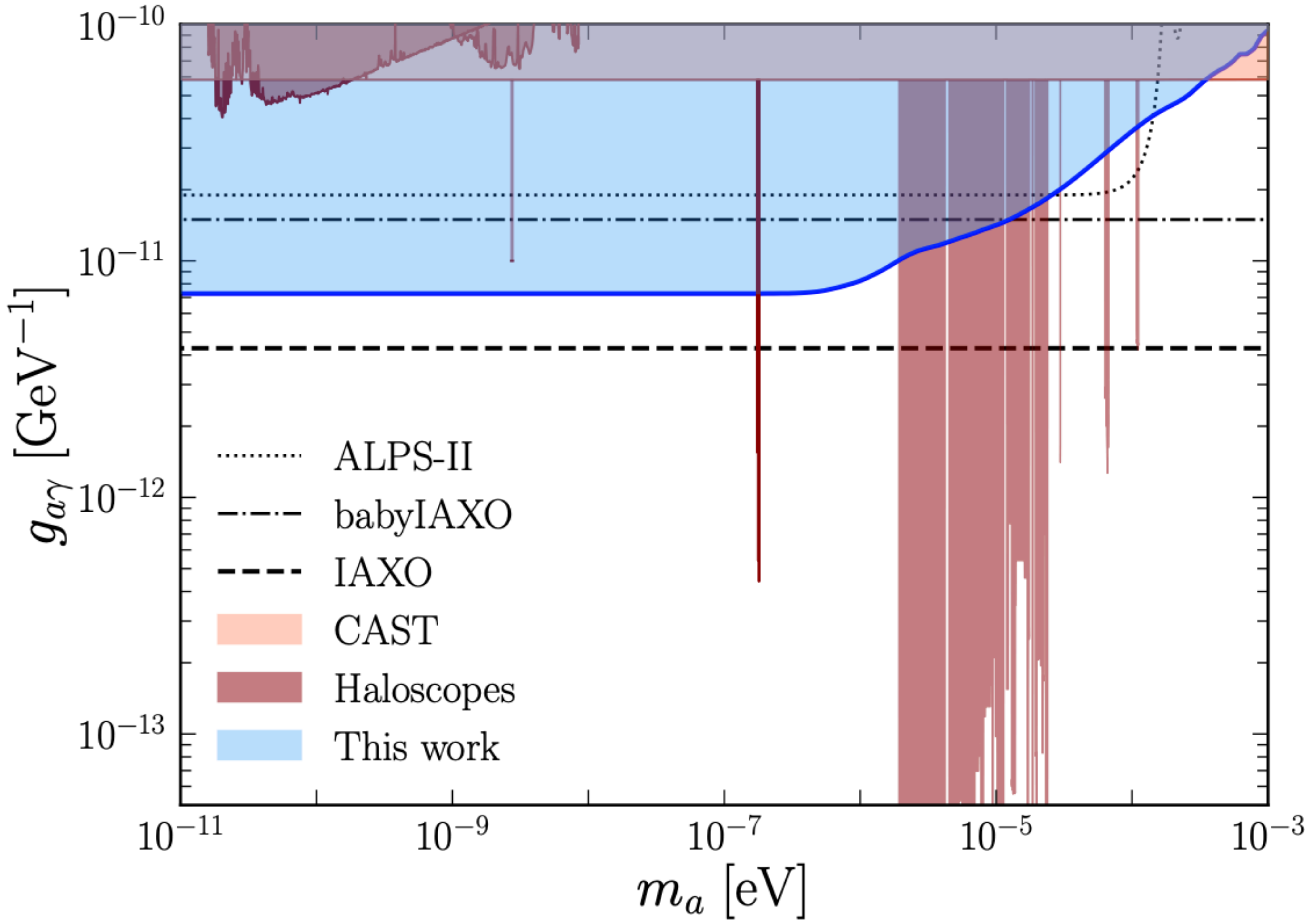
10^{-10}
10^{-11}
10^{-12}
10^{-13}
$g_{a\gamma}$ [GeV^{-1}]
10^{-11}
10^{-9}
10^{-7}
10^{-5}
10^{-3}
m_a [eV]
ALPS-II
babyIAXO
IAXO
CAST
Haloscopes
This work